land

MDPI

Article

Acceleration of Soil Erosion by Different Land Uses in Arid Lands above ^{10}Be Natural Background Rates: Case Study in the Sonoran Desert, USA

Ara Jeong [1,*], Ronald I. Dorn [2], Yeong-Bae Seong [1] and Byung-Yong Yu [3]

[1] Department of Geography Education, Korea University, Seoul 02841, Korea; ybseong@korea.ac.kr
[2] School of Geographical Sciences and Urban Planning, Arizona State University, Tempe, AZ 85287, USA; atrid@asu.edu
[3] Laboratory of Accelerator Mass Spectrometry, Korea Institute of Science and Technology, Seoul 02792, Korea; yu2997@kist.re.kr
* Correspondence: ara0408@korea.ac.kr

Abstract: Land use changes often lead to soil erosion, land degradation, and environmental deterioration. However, little is known about just how much humans accelerate erosion compared to natural background rates in non-agricultural settings, despite its importance to knowing the magnitude of soil degradation. The lack of understanding of anthropogenic acceleration is especially true for arid regions. Thus, we used ^{10}Be catchment averaged denudation rates (CADRs) to obtain natural rates of soil erosion in and around the Phoenix metropolitan region, Arizona, United States. We then measured the acceleration of soil erosion by grazing, wildfire, and urban construction by comparing CADRs to erosion rates for the same watersheds, finding that: (i) grazing sometimes can increase sediment yields by up to 2.3–2.6x, (ii) human-set wildfires increased sediment yields by up to 9.7–10.4x, (iii) after some post-fire vegetation recovered, sediment yield was then up to 4.2–4.5x the background yield, (iv) construction increased sediment yields by up to 5.0–5.6x, and (v) the sealing of urban surfaces led to one-tenth to one-half of the background sediment yields. The acceleration of erosion at the urban–rural interface in arid lands highlights the need for sustainable management of arid-region soils.

Keywords: ^{10}Be denudation rates; arid lands; grazing; land use changes; land degradation; natural background rate; soil erosion; wildfire; urban construction

Citation: Jeong, A.; Dorn, R.I.; Seong, Y.-B.; Yu, B.-Y. Acceleration of Soil Erosion by Different Land Uses in Arid Lands above ^{10}Be Natural Background Rates: Case Study in the Sonoran Desert, USA. *Land* **2021**, *10*, 834. https://doi.org/10.3390/land10080834

Academic Editors: Artemi Cerdà, Erick R. Bandala, Yang Yu and Jesús Rodrigo-Comino

Received: 25 July 2021
Accepted: 4 August 2021
Published: 9 August 2021

1. Introduction

The scholarly study of soils and their geographical variability rests at the nexus of a variety of disciplines, including agronomy, botany, geology, forestry, planning and development, religious studies, the Soviet tradition of landscape science, water science and technology, and, at its core, physical geography [1,2]. Soil erosion studies are just as interdisciplinary, as reflected in a recent analysis of citation patterns [3]. This high level of interest in soils and soil erosion can be explained by the critical functions and services for societies and natural environments that soils provide [4–9].

A fundamental reality is that soils develop over 10^3–10^6 year timescales [10]. Yet, land use land cover changes (LULCCs) on timescales of 10^1–10^2 years greatly increase soil erosion [11–26]. Unfortunately, the continued existence of soils requires that the rate of replenishment be equal to or greater than the rate of erosion [27].

Cosmogenic nuclides have revolutionized the study of earth surface processes [28], including soil erosion, by analyzing the cosmogenic nuclide ^{10}Be in quartz at the mouths of catchments [10,27]. Catchment averaged denudation rates (CADRs) provide an understanding of erosion rates over timescales of 10^3–10^5 years. This allows for comparisons between modern and natural background erosion rates. For example, agricultural fields erode soils 1–2 orders of magnitude greater than natural rates [29,30].

Poesen [31] advocated for the importance of research to develop a better understanding of both natural and anthropogenic soil erosion. Thus, here, we compare modern rates of soil erosion to natural background rates (CADRs). Our regional focus is the northeast Sonoran Desert of western North America—the area in and around the Phoenix metropolitan region (PMR), Arizona, United States [32]. Prior research [33] analyzed over two decades of soil erosion in the PMR, comparing the impacts of urbanization, wildfire, and grazing—key processes leading to soil erosion (urban construction [22]; wildfires [34,35]; and overgrazing [36]). Nearing et al. [37] reviewed natural and anthropogenic rates of soil erosion in the United States and northeastern China using geologic rates of soil erosion that included ^{10}Be CADRs. Here, we focus our research on the exact same catchments where we obtain background rates of soil erosion from CADRs and also modern soil erosion from urbanization, wildfire, or grazing in an arid region.

2. Study Area

The Sonoran Desert in central Arizona (Figure 1) is classified as having a Köppen–Geiger climate. A 100-year climate record (1895–1998 CE) from Phoenix, Arizona, United States shows that the annual precipitation averages 202 mm and the average temperatures range from 6 °C in January to 41 °C in July [38]. Bimodal rainfall occurs in winter (November to March) from cold fronts and in July and August from the North American monsoon [39].

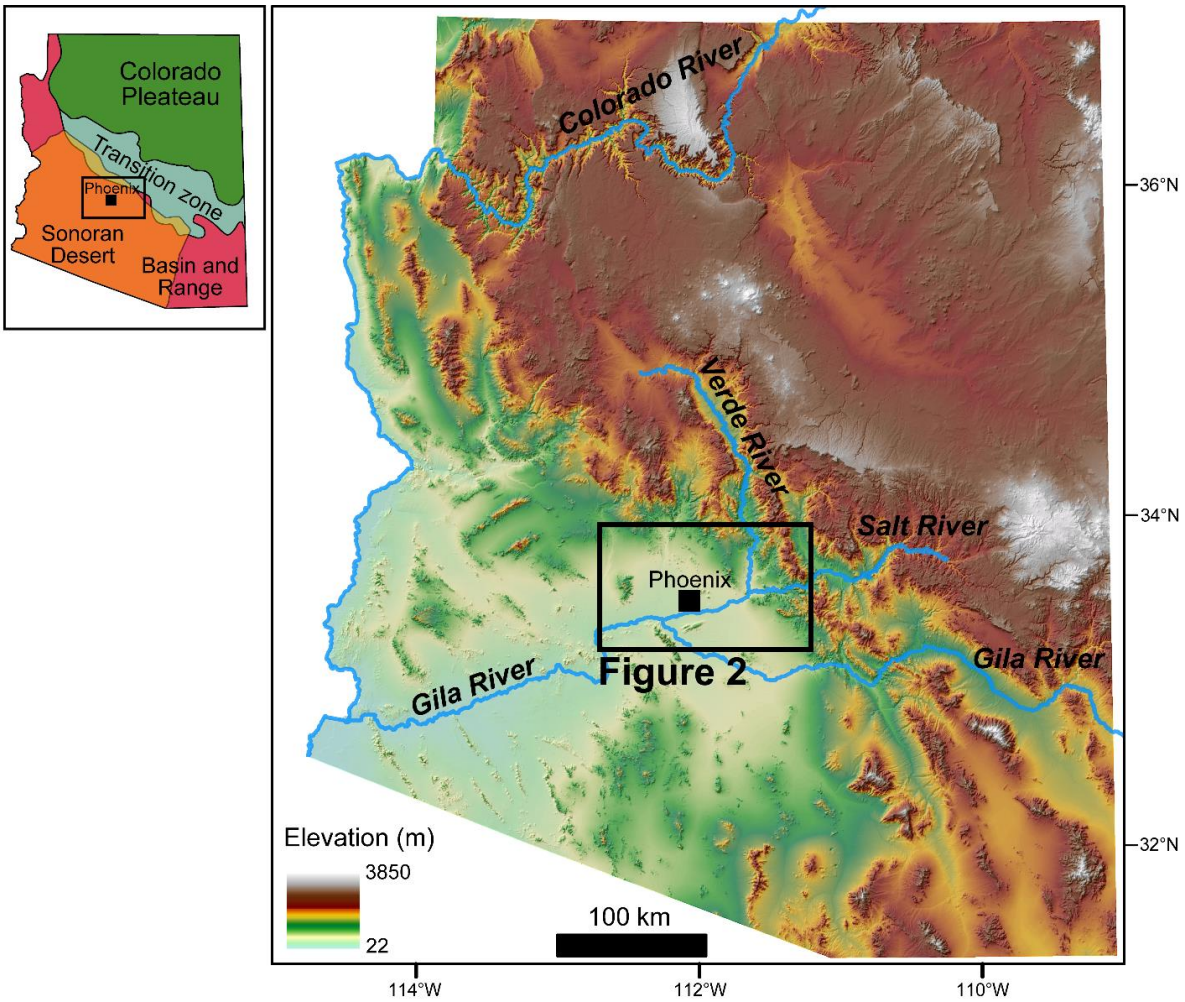

Figure 1. Topography of Arizona, United States with the studied watersheds found within the box. This study area occurs in the climatological Sonoran Desert and within a geological Basin and Range Province where the Salt, Verde, and Gila rivers flow through the Phoenix metropolitan region, Arizona, United States.

Our research focuses on 18 stock ponds located on the margins of Phoenix's urban sprawl (Figure 2). Berms were constructed in the 1950s and 1960s, blocking small drainages in order to collect water for cattle. We previously collected data from over two decades of soil erosion in the small watersheds of these stock ponds as well as monitored land use land cover changes (LULCCs), including grazing, wildfires, and urban construction [33]. For this study, we collected CADR samples from these same catchments to permit a direct comparison between modern and natural erosion rates. Our strategy of using artificial dams is certainly not unique. Vaezi et al. [40], for example, calculated the sediment yield in twenty small catchments by measuring the sediment mass that accumulated behind check dams in northwest Iran.

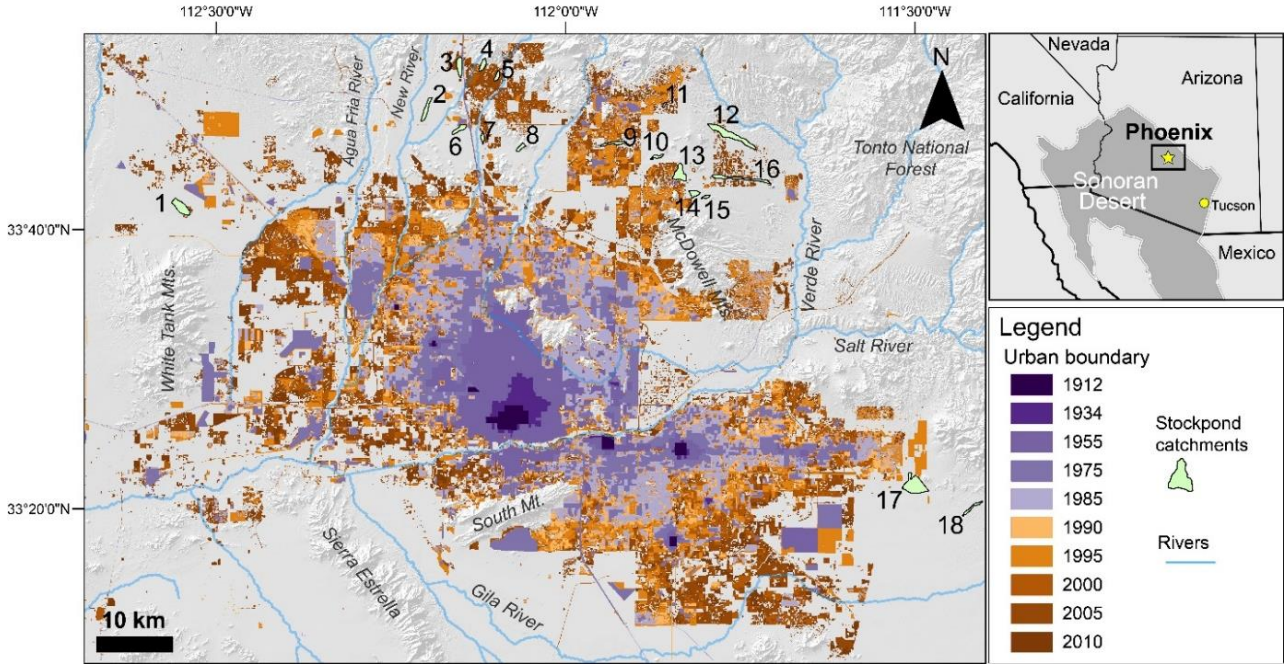

Figure 2. The urban sprawl of the Phoenix metropolitan region from 1912 to 2010 provides context for the locations of the 18 monitored stock pond catchments in the Sonoran Desert, United States. Urban boundaries were extracted from a land cover classification by Central Arizona–Phoenix Long-Term Ecological Research. Numbers match to the stock ponds identified in Tables 2 and 4.

This study site section places the 18 stock pond study sites (Figure 3) within the context of broader issues of soil erosion in the Phoenix metropolitan region (PMR). Similar to Mohammed et al.'s study [41] in Syria, Jeong and Dorn [33] found that different LULCCs in the PMR increased historic erosion rates. Thus, this section provides regional background on the key PMR LULCCs of (i) grazing; (ii) wildfires; and (iii) exposure of bare ground due to urbanization.

Grazing impacts erosion processes in our watersheds by reducing vegetation cover and by the removal of biological soil crusts (BSCs) that once protected desert surfaces from wind and water erosion [42,43]. Naturally, BSCs were much more extensive in the region [44], but currently remain only as isolated patches—all due to human-induced disturbances such as cattle grazing [32]. The removal of BSCs means that the dominant processes of grain detachment and transport that we observed directly during the two-decade study were rainsplash [45] and overland flow.

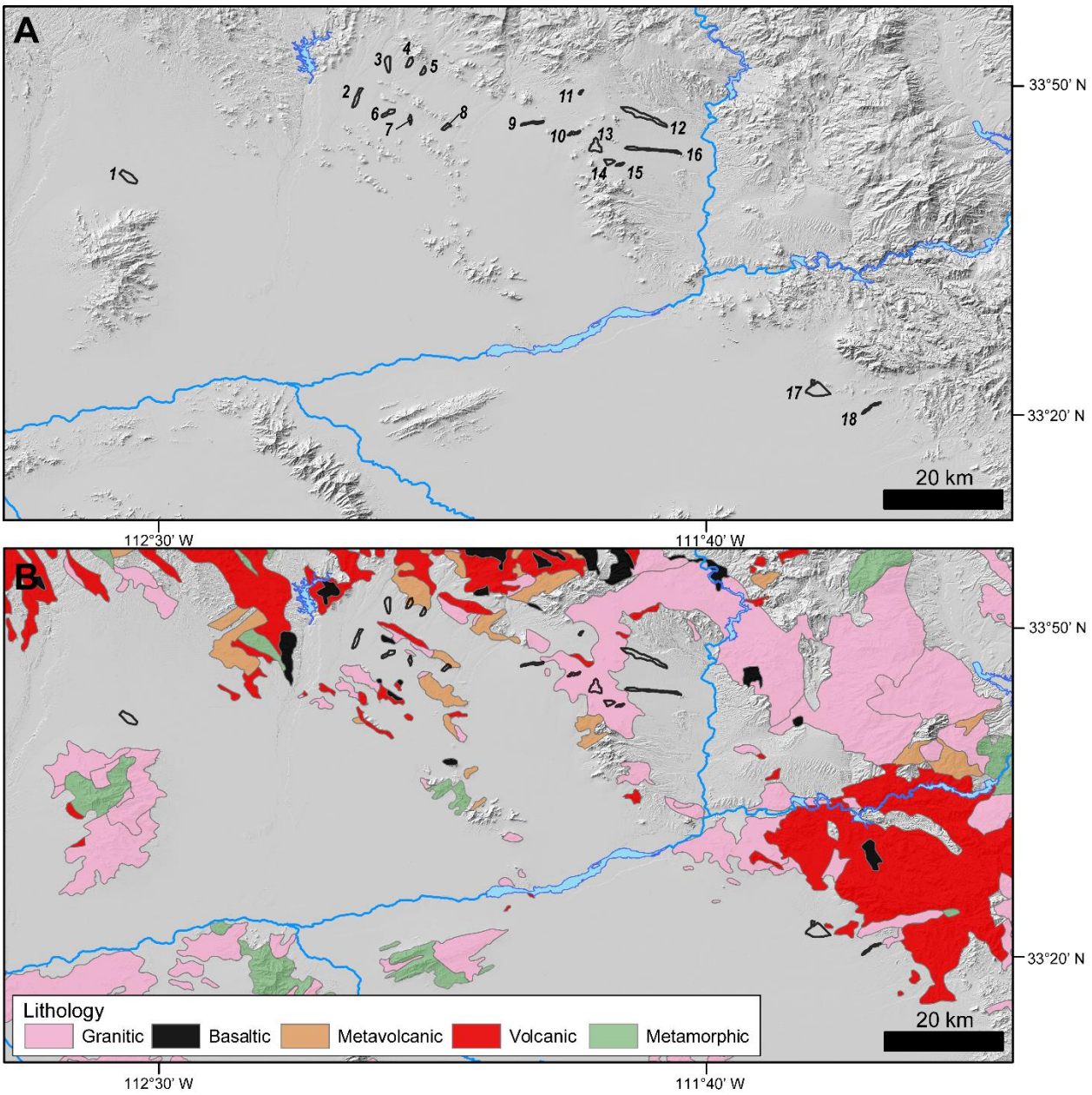

Figure 3. Metropolitan Phoenix, framed by the box in Figure 1. (**A**) Location of catchments studied by ^{10}Be CADRs where numbers correspond to Tables 3 and 6. (**B**) Basic geologic map of the composition of bedrock ranges. The study sites are located on piedmonts of these ranges, both pediments and alluvial fans, experiencing urban sprawl.

Gullying is a key soil erosion process [20,46,47]. However, we did not observe gullying during our two decades of field observations in the studied watersheds [33]. Similarly, slope can be a critical control on soil erosion [41,48,49]. Jeong and Dorn [33], however, did not find a statistically significant correlation between sediment yield and typical catchment properties, including slope, relief, drainage area, and drainage density, with possible reasons being the greater importance of LULCCs and also relatively small differences in these morphometric factors between the different PMR catchments.

Wildfire did not occur naturally in the Sonoran Desert during the Holocene [50]. Even though lightning strikes occur in the region during the North American monsoon summer season, sparse vegetation cover naturally inhibited the spread of fires in the Sonoran Desert [50]. This condition changed with the invasion of exotic annual grasses such as *Bromus tectorum* and *Bromus madritensis* ssp. *Rubens* that altered natural grass/fire

cycles [51]. For example, D'Antonio and Vitousek [52] reported that the replacement of native shrublands by invasive grasses produced an abundance of fuels followed by an increasing frequency of large fires. Furthermore, after fires, invasive grasses typically thrive, leading to a fire regime that did not previously exist naturally [53]. Along with the urban sprawl's encroachment on our studied catchments (Figure 1) came enhanced recreation by the urban population, including gun target shooting, off-road vehicle use, and, in particular, cigarette smoking by these users—a formula for wildfires that periodically consumed the studied watersheds.

With the advent of air conditioning, after World War II, the PMR rapidly expanded due to migrants seeking work, affordable housing, health in the warm dry desert, retirement, and an outdoor lifestyle [54]. Urban expansion mapped in Figure 2 prior to the 1950s took place on flat agricultural fields. Subsequent urban sprawl creeped out onto the piedmonts of desert mountain ranges, both pediments and alluvial fans [32]. The 18 stock pond watersheds (Figures 2 and 3) are located on pediments and fans with a variety of rock types (Figure 3). Urban sprawl in the Sonoran Desert (Figure 2) increased the region's vulnerability to erosion through construction, exposing bare ground to rainfall and runoff [32,55].

3. Materials and Methods

The first two parts of this section detail our approach to measuring background CADRs, first testing whether human-induced erosion impacts CADRs in the Sonoran Desert and then measuring CADRs for each of the 18 PMR catchments. The third part of this section then explains a statistical analysis of CADRs and morphometric characteristics of the catchments. The last part summarizes modern sediment yield data presented in detail in Jeong and Dorn [33] and how we compare those data with CADRs for the same catchments.

3.1. Test Experiment for Assessing the Effect of Human Activities on CADRs

The general observation amongst geomorphologists using ^{10}Be to measure rates of erosion is that human activities do not influence CADRs [56]. This observation was true in a study of a mountainous watershed in the Phoenix area [57]. However, we felt it prudent to test whether aggressive urbanization in the form of a housing development might generate enough sediment to alter CADRs. Thus, we designed an experiment.

The idea of this test was to find a watershed that had its upper region in a natural preserve with a lower region experiencing rapid urbanization. In addition, the idea was for the watershed to have slopes that were on the steeper end of the Phoenix area, in order to accelerate potential differences in CADRs. In other words, if the CADR technique could be impacted by modern soil erosion, it would be in a location with steep slopes turned bare by bulldozers plowing a big subdivision.

Figure 4 presents our conceptual model for the experiment. In this idealized catchment, natural land cover occupies the upper-subcatchment and urban land cover occupies the lower-subcatchment. When the other controls on CADRs are the same for these two catchments (e.g., geology, no mass wasting), only land cover is the variable that might impact CADRs. We sampled an ideal catchment on a desert piedmont for this experiment in March of 2016, and we collected sediment samples from the main wash (CAPC01), from an upper-subcatchment where the city of Phoenix has a Sonoran Preserve (CAPC02), and from a lower sub-catchment with active clearing of land for a subdivision (CAPC03). The major rock type in this catchment is consistently Early Proterozoic Metavolcanic Rocks. Therefore, we can exclude the impact of rock type on CADRs. Figure 5 provides insight about the surface condition of the sampling locations.

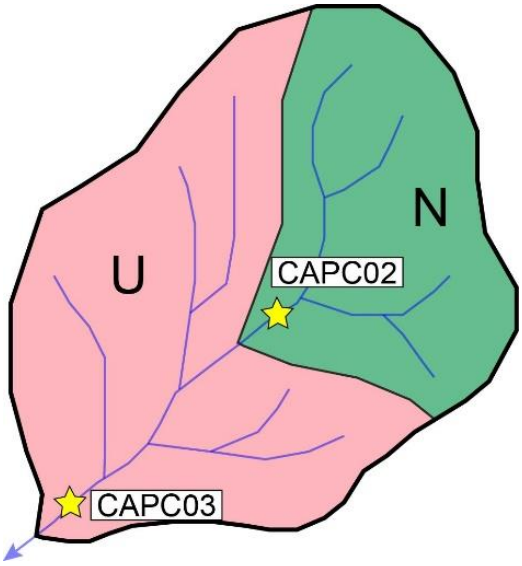

Figure 4. Conceptual model of a controlled experiment to determine if the CADR is influenced by urban construction in the Phoenix area. N refers to natural land cover and U refers to urban land cover. The sediment sample collected from the upper-subcatchment (CAPC02) represents the CADR of a nature preserve setting, while the sediment sample collected from the lower-subcatchment (CAPC03) represents the CADR impacted by a highly disturbed catchment that was experiencing ongoing suburbanization through the creation of a subdivision.

3.2. Natural Background Sediment Yield Derived from ^{10}Be

We collected samples of active-channel sediment from each of the 18 studied catchments that experienced LULCCs in the last two decades [33] to measure CADRs on the Sonoran Desert piedmont (Figures 2 and 3). All of the drainage networks in these 18 Phoenix-region catchments combine into a single channel that transfers sediment to the stock pond. CADR samples were all collected from this single channel just above each stock pond.

After sieving the collected fluvial sediments, just the 250–750 μm size fraction was chemically treated [58] at the Geochronology Laboratory at Korea University, Seoul, Korea. The treatment repeatedly etches minerals in a dilute HF/HNO_3 mixture [58]. We added a ^{9}Be carrier with a $^{10}Be/^{9}Be$ ratio $< 3.0 \times 10^{-15}$, then separated and purified the Be by ion exchange chromatography and selective precipitation of BeOH at pH > 7. BeOH was oxidized by ignition in a quartz crucible at 800 °C for 10 min [59]. BeO was then mixed with Nb metal and loaded onto targets for the measurement of the $^{10}Be/^{9}Be$ ratio by the 6MV accelerator mass spectrometer (AMS) at the facility of the Korean Institute of Science and Technology (KIST), Seoul, Korea [59]. Isotope ratios were normalized to the ^{10}Be standards [60], and the measured isotope ratios were converted to cosmogenic ^{10}Be concentrations in quartz using the total ^{10}Be in the samples and sample weights.

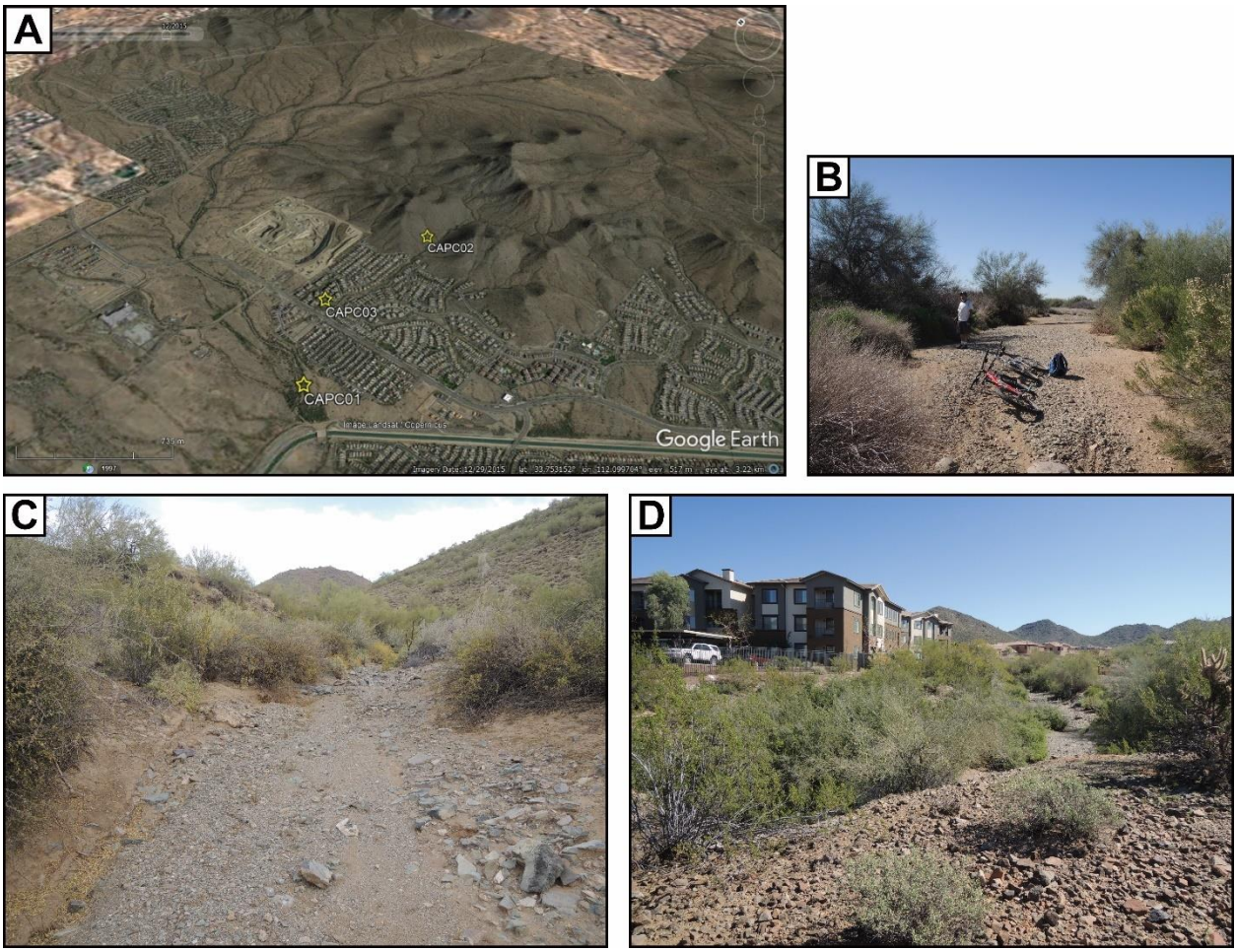

Figure 5. Study sites of the experiment to assess if the CADR is impacted by urbanization. (**A**) Google Earth view showing sampling locations and different land uses in the controlled experiment catchment. (**B**) Sampling location of the CAPC01 sample. (**C**) Sampling location of the CAPC02 sample. The CAPC02 subcatchment is within the Sonoran Preserve. (**D**) Sampling location of the CAPC03 sample, where the land surrounding CAPC03 was either recently built homes or bare ground.

We calculated the CADRs using the CRONUS online calculator (version 2.2) [61], which calculates the ^{10}Be production rate by integrating shielding conditions and latitude–altitude production rate functions [62–65]. CADR erosion rate calculations assume a bedrock bulk density of 2.7 g cm^{-3}. In order to calculate the background-area-specific sediment yield represented by mass per unit area per time, we converted the CADR measured as length per time into the same unit of area-specific sediment yield (Mg km^{-2} yr^{-1}) using a bedrock density of 2.7 g cm^{-3}. Specifically, the background-area-specific sediment yield (SSY) was calculated using the following equation:

$$\text{Background SSY} = \text{CADR} \times \rho \quad (1)$$

where SSY is Mg km^{-2} yr^{-1}, CADR is m Myr^{-1} (=10^{-3} km 10^{6} yr^{-1}), and ρ is g cm^{-3} (=10^{-6} Mg 10^{-15} km^{3}). An example of the conversion follows for the Cigar site: the background SSY is calculated as 7.1 m Myr^{-1} × 2.7 g cm^{-3}.

3.3. Correlation between Geomorphic Catchment Properties and Background Erosion Rate

We gathered quantitative and qualitative data for each of the selected catchments to determine if there were statistically significant correlations between a catchment property and natural background rates of erosion from the CADR. The morphological variables, such

as drainage area, mean slope, and maximum relief, were generated by ArcGIS software using a 10 m DEM. Data on rock type were extracted from the geologic map provided by USGS (https://mrdata.usgs.gov/geology/state/state.php?state=AZ, accessed on 8 April 2021). Mean annual precipitation (MAP) and rainfall intensity were calculated using the precipitation data from various rain gauges of the Maricopa County Flood Control District (http://alert.fcd.maricopa.gov/showrpts_mc.html, accessed on 8 April 2021). In the semiarid watershed of southern Arizona, the sediment transport is generated when the rainfall intensity is greater than 10 mm for 30 min (I30) [66]. Therefore, rainfall intensity was calculated based on the I30. In addition, the 10-year average MAP and I30 (Period 1: 1989–1999; Period 2: 2000–2009) are presented to reduce the effect of short-term variances in rainfalls. Jeong and Dorn [33] present detailed information on the various catchment properties analyzed here.

We excluded two of our observed natural background sediment yields from the bivariate correlation tests. These two watersheds had comparatively steep catchment mean slopes (6.6° and 6.2°) because the residential development backed up against mountain desert slopes. Generally, in Phoenix, residential development rarely occurs on this steep-slope terrain, because of the abundance of alluvial fans and pediments with lower slopes. Because these two watersheds are influenced strongly by the presence of backing desert mountains, we omitted them from the correlation analysis in order to avoid bias.

Since rock types are not ordinal data, we completed analyses of Student's *t*-tests to understand the importance of rock type on natural background sediment yield. Half of the stock pond watersheds are underlain by only granitic lithologies, ranging from granite to granodiorite with some diorite; the other half of the stock pond watersheds are underlain by a mix of rock types, typically including rhyolitic tuff (ignimbrite), basalt, metavolcanic, and metasedimentary rocks (Figure 3).

3.4. Modern Sediment Yield

The premise of this paper rests in comparing natural rates of erosion (CADRs) to prior research that analyzed two decades of historic erosion associated with LULCCs. This section summarizes the approach used to collect those historic erosion data presented in Jeong and Dorn [33].

Sediments collected from 18 stock ponds monitored soil erosion as the Phoenix urban fringe expanded between 1989 and 2013 [33]. A Supplementary Google Earth File linked with the main paper submission presents the 18 studied stock pond watersheds. The selection of the stock ponds to monitor was based on obtaining local information that a land-use change was planned from the prior use of cattle grazing. Sometimes, that land-use change did not occur or did not take place on the anticipated timescale. The result is a mixture of land-use changes impacting sediment yields as the Phoenix metropolitan area expanded (Figure 6). We stress that these areas are not susceptible to gullying or streambed erosion processes, and that sediment derives from mobilization of gravel and finer sediment by rainsplash and overland flow processes that sometimes involve rilling up to 5 cm in depth.

In each stock tank, nine 0.3 m segments of steel rebar were pounded flush to the surface of the sediment accumulation area in a 3 × 3 grid to account for spatial variability in sedimentation. Stock ponds were revisited at each major land use change to measure sediment accumulation depths on top of the rebar, located using a metal detector. Bulk density samples were collected from three points at each monitoring event and determined using the hydrometer method with the reported error term from the standard deviation. We estimated the maximum erosion rate with assumptions that all of the silt and clay derived from the local watershed, whereas the minimum erosion rate assumes that all of the silt and clay derived from aeolian deposition.

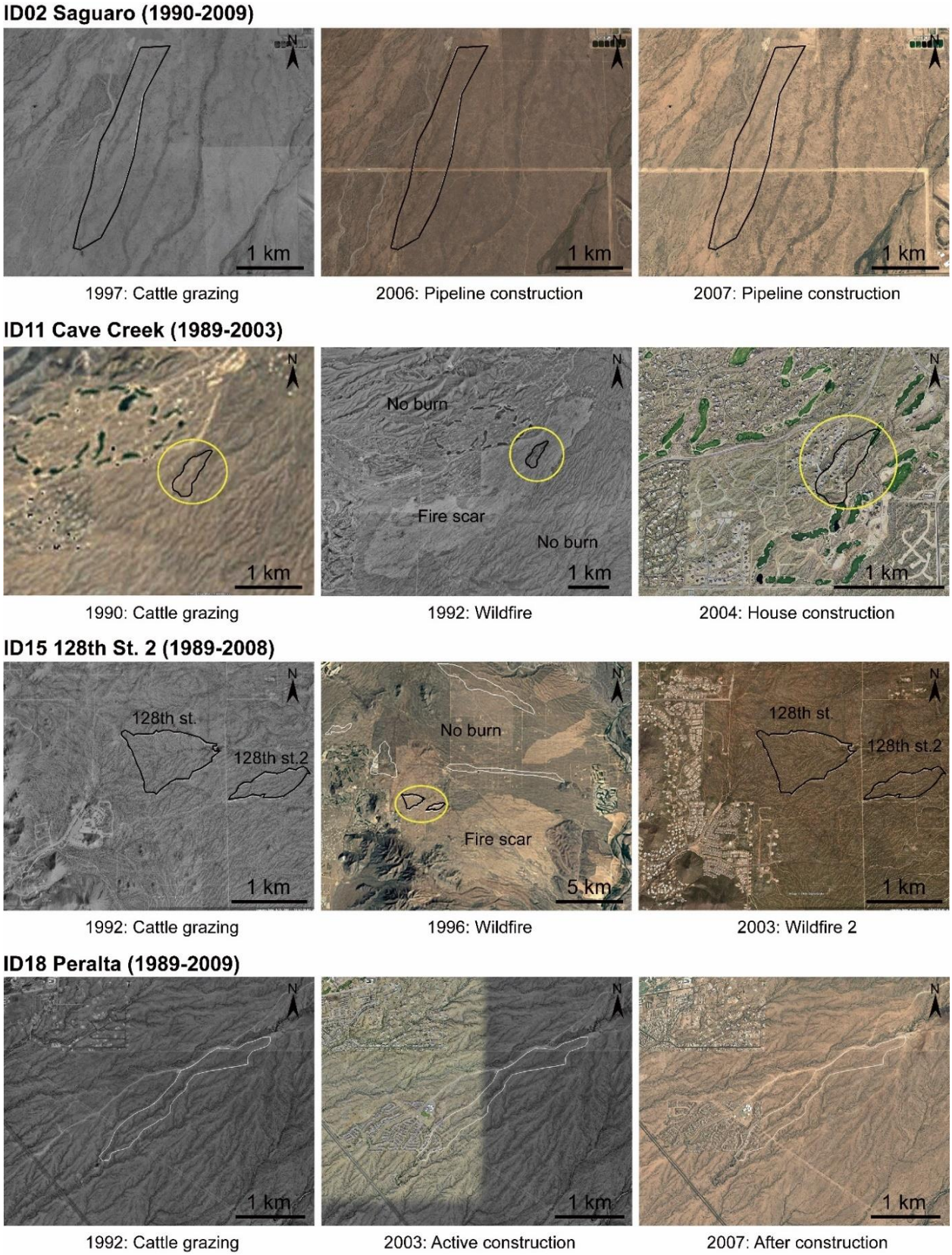

Figure 6. Historic aerial photography showing the typical land-use changes in four stock pond watersheds. The ID numbers correspond with the numbers in the figures and tables of this paper.

3.5. Comparison between Modern Sediment Yield and CADR

Most geomorphologists utilizing cosmogenic nuclides think about CADRs or natural rates of erosion in terms of millimeters per thousand years. Thus, the unit of CADR is different than soil erosion measurements, whether the audience involves scientists or policy-makers [67–69]. A key issue that needs to be resolved is to decide the most widely applicable unit to measure the sediment yield that results from soil erosion. Thus, the purpose of this section rests in clarifying our decision to present all sediment yield data in terms of area-specific sediment yield (Mg km^{-2} yr^{-1}).

In general, sediment yield represents the amount of sediment that has been transported from one location to another measured as mass per time or volume per time or mass per unit area per time. The exact definition, however, can vary from country to country, among governmental agencies, and among different researchers (Table 1 (1-1)).

Table 1 (1-2) illustrates how soil erosion or sediment yield models vary in their data presentation. Universal Soil Loss Equation (USLE)-type models (USLE, RUSLE, and MUSLE) were designed to predict soil erosion on either plot scale or catchment scale, so they use the term average annual soil loss as represented by mass per unit area per time, which is often incorporated into other sediment yield models. Sediment yield models (SWAT, AGNPS, and WEPP) differentiate soil erosion and sediment yield by adding a sediment delivery ratio term into their model. These models report the sediment yield result as either mass per time or mass per unit area per time (Table 1 (1-2)). Although the output of USLE-type models is different from other sediment models, cross-comparisons exist between USLE-type models and other sediment models [70,71].

Natural background rates use the CADR approach, and this scholarship takes two approaches (Table 1 (1-3)). One strategy converts modern area-specific sediment yield (Mg km^{-2} yr^{-1}) to a CADR (m Myr^{-1}) by dividing bedrock density (2.6–2.7 g cm^{-3}) [72,73]. Another CADR approach calculates background-area-specific sediment yield by multiplying bedrock density and then comparing it to modern sediment yield correcting for sediment bulk density (1.x g cm^{-3}) [71,74,75] (Table 1 (1-3)). We adopted the latter to compare natural background and modern sediment yield data.

Table 1. Different approaches to reporting sediment yield.

1 (1-1). Different approaches to representing the amount of sediment that has moved from its original site			
Agency	**Reported term**	**Unit**	**Reference**
Food and Agriculture Organization of the United Nations	Annual sediment yield	$[M\ L^{-2}\ T^{-1}]$ ($t\ km^{-2}\ yr^{-1}$)	FAO [76]
U.S. Department of the Interior, Bureau of Reclamation	Sediment yield	$[M\ T^{-1}]$, $[L^3\ T^{-1}]$ ($tons^{-1}\ yr^{-1}$), ($m^3\ yr^{-1}$)	USBR [77]
U.S. Department of the Interior, Bureau of Reclamation	Sediment yield rate	$[M\ L^{-2}\ T^{-1}]$, $[L^3\ L^{-2}\ T^{-1}]$ ($m^3\ km^{-2}\ yr^{-1}$) (ac ft $mi^{-2}\ yr^{-1}$)	Strand and Pemberton [78]; USDA [79]
U.S. Department of Agriculture Natural Resources Conservation Service (USDA-NRCS)	Sediment yield	$[M\ T^{-1}]$ ($tons\ yr^{-1}$)	Wischmeier and Smith [80]
EUROPEAN SOIL DATA CENTRE (ESDAC)	Sediment yield	$[M\ T^{-1}]$ ($Pg\ yr^{-1}$)	Borrelli et al. [81]
EUROPEAN SOIL DATA CENTRE (ESDAC)	Area-specific sediment yield	$[M\ L^{-2}\ T^{-1}]$, ($Mg\ ha^{-1}\ yr^{-1}$)	Borrelli et al. [81]
1 (1-2). Soil erosion and sediment yield models			
Model Name	**Reported term**	**Unit**	**Reference**
Universal Soil Loss Equation (USLE), Revised Universal Soil Loss Equation (RUSLE)	Average annual soil loss	$[M\ L^{-2}\ T^{-1}]$, ($tons\ acre^{-1}\ yr^{-1}$)	Wischmeier and Smith [80,82]
Soil and Water Assessment Tool (SWAT)	Sediment yield	$[M\ L^{-2}]$, ($t\ ha^{-1}$),	Arnold et al. [83]
AGricultural Non-Point Source Pollution Model (AGNPS)	Eroded sediments Sediment yield for catchment	$[M\ L^{-2}]$, ($tons\ acre^{-1}$) [M], (tons)	Young et al. [84]
Water Erosion Prediction Project (WEPP)	Average annual soil loss Average annual sediment yield	$[M\ L^{-2}\ T^{-1}]$, ($ton\ acre^{-1}\ yr^{-1}$)	Laflen et al. [85]

Table 1. *Cont.*

1 (1-3). CADR scholarship comparing the CADR-derived background rate (time scale: 10^3–10^5) to the modern rate (time scale: 10^0–10^2)				
Approach	**Background rate**	**Modern rate**	**Unit**	**References**
1. Convert the modern area-specific sediment yield (SSY) to the erosion rate using bedrock density (2.6–2.7 g cm^{-3})	Catchment averaged denudation rate (CADR)	Erosion rate (Area-specific sediment yield / Bedrock density (2.6–2.7 g cm^{-3}))	[L T^{-1}], (m Myr^{-1})	Schaller et al. [72]; Bierman et al. [73]
2. Convert the CADR to the SSY using bedrock density (2.6–2.7 g cm^{-3})	Area-specific sediment yield (CADR bedrock density (2.6–2.7 g cm^{-3}))	Area-specific sediment yield calculated using sediment density (1.x g cm^{-3})	[M L^{-2} T^{-1}], (Mg km^{-2} yr^{-1}) (kg m^{-2} yr^{-1})	Hewawasam et al. [74] [a]; Clapp et al. [75] [b] Gellis et al. [86] [c] This study

[a] Did not refer "density" to calculate the modern sediment yield, but described modern sediment as deriving from river gauge and reservoir measurements. [b] used sediment density: 1.6 g cm^{-3}. [c] only mentioned that they used sediment density to calculate the sediment yield.

4. Results

The results section first reveals that aggressive urbanization processes in the Sonoran Desert do not appear to influence CADR measurements. This is followed by our CADR findings of natural background erosion rates for the 18 stock pond catchments, as well as the results of a correlation analysis comparing the CADR to various properties of the catchments. The third section then turns to a comparison between CADRs and modern rates of erosion to quantify the acceleration of erosion above the natural background by different LULCCs.

4.1. Influences of Recent Disturbances on CADRs

Although anthropogenic disturbances changed the surface condition and accelerated historical erosion in the Sonoran Desert [33], the influence of housing development on the ^{10}Be CADR is below the limit that we can detect, resting at <10% in central Arizona—within in the external error range (Table 2), which follows the same pattern as in other global locations [56,57]. This finding suggests that ^{10}Be CADR can represent natural background rates of erosion and can be used as a baseline for comparison with human-impacted erosion. Future researchers should be aware that our conclusion would not apply if the scale of anthropogenic erosion "mines" minerals below the cosmic ray penetration depth of ~60 cm.

Table 2. Catchment averaged denudation rates (CADRs) in the controlled experiment based on cosmogenic ^{10}Be analyses. Sample ID number corresponds to the sampling locations that are presented in Figure 4. The CAP02 sample comes from the preserve, while CAP03 comes from the subdivision. The CAP03 sample integrates a larger drainage area that mixes preserve and development land uses.

Sample ID	Latitude (°N)	Longitude (°W)	Elevation (m asl)	Production Rate (Atoms g^{-1} yr^{-1}) [a]	Blank-Corrected [^{10}Be] ± 1σ (10^5 Atoms g^{-1}) [b]	^{10}Be Erosion rate ± 1σ (m Myr^{-1}) [c]	^{10}Be Sediment Yield ± 1σ (Mg km^{-2} yr^{-1}) [d]	Timescale ± 1σ (kyr) [e]
CAPC01	33.7494	112.1136	489	5.81	3.04 ± 0.04	11.0 ± 0.1	29.8 ± 0.3	53.7 ± 0.6
CAPC02	33.7512	112.0984	527	5.92	2.37 ± 0.03	14.5 ± 0.2	39.2 ± 0.5	40.8 ± 0.5
CAPC03	33.7526	112.01078	508	5.87	2.42 ± 0.03	14.1 ± 0.2	38.1 ± 0.5	42.0 ± 0.5

[a] Total catchment averaged production rates were calculated using the CRONUS calculator (v 2.2) [61], which includes spallogenic and muogenic production. The reference production rate for sea-level and high latitude is 4.49 atoms g^{-1} yr^{-1} [63]. [b] Normalized with standard 07KNSTD and corrected for process blank. Error propagation was based on Balco et al. [61]. A large value between the internal error and the external error was selected. [c] Background sediment yield was calculated using Equation (1). [d] Beryllium-10 erosion rates were calculated using the CRONUS calculator (v 2.2) [61], assuming a bedrock density ρ = 2.7 g cm^{-3}. [e] Timescale of the catchment averaged denudation rate wes calculated by dividing the 10Be concentration by the total production rate, which accounts for the duration over which a depth of $z^* = \Lambda/\rho \sim 60$ cm surface in the eroded basin.

4.2. Cosmogenic Nuclide ^{10}Be-Derived CADR

Table 3 provides CADRs of each stock pond watershed (see Figure 2 for the location of each stock pond watershed). Table 3 presents details of each site needed to calculate production rates, the AMS measurement of the ^{10}Be concentration, the calculation of the CADR in meters per million years, the residence timescale of the sediment in each catchment in thousands of years, and the calculation of natural background sediment yields.

A correlation matrix presents Pearson's correlation coefficients between the natural background sediment yield and morphometric properties of each catchment (Table 4). Natural background sediment yield was significantly and positively correlated with mean slope ($r = 0.75$, $p < 0.05$) and mean elevation ($r = 0.63$, $p < 0.05$), but drainage area, relief, and drainage density did not show a clear correlation. Mean slope and mean elevation are significantly and positively correlated ($r = 0.8$, $p < 0.05$).

Table 3. CADRs based on cosmogenic ^{10}Be analyses. The sample ID corresponds to the different watersheds in the Phoenix Metropolitan Region (PMR) that are presented in Figure 2.

Sample ID	Latitude. (°N)	Longitude (°W)	Mean Lat. [a] (°N)	Mean Long. [a] (°W)	Elevation (m asl)	Avg. Basin Slope (°)	Production Rate (Atoms g^{-1} yr^{-1}) [b]	Blank-Corrected [^{10}Be] ± 1σ (10^5 Atoms g^{-1}) [c]	^{10}Be Erosion Rate ± 1σ (m Myr^{-1})	^{10} Be Sediment Yield ± 1σ (Mg km^{-2} yr^{-1})	Timescale ± 1σ (kyr) [d]
1. Cigar	33.685	112.534	33.696	112.547	462	0.4	5.88	5.85 ± 0.06	7.1 ± 0.6	19.3 ± 1.5	99.5 ± 1.1
2. Saguaro	33.801	112.204	33.816	112.197	496	0.7	6.04	3.74 ± 0.05	12.1 ± 0.9	32.7 ± 2.4	62.0 ± 0.8
3. Cline	33.856	112.149	33.867	112.152	568	1.2	6.39	6.46 ± 0.08	6.9 ± 0.6	18.7 ± 1.5	101.1 ± 1.2
4. Anthem	33.851	112.102	33.870	112.117	611	6.2	6.59	2.62 ± 0.04	19.4 ± 1.4	52.2 ± 3.8	39.7 ± 0.6
5. Anthem 2	33.852	112.100	33.857	112.097	586	1.8	6.46	1.89 ± 0.03	27.0 ± 1.9	73.0 ± 5.2	29.3 ± 0.5
6. Pepe	33.786	112.160	33.792	112.150	495	0.6	6.03	5.19 ± 0.06	8.4 ± 0.6	22.6 ± 1.7	86.0 ± 1.0
7. Bronco	33.775	112.117	33.783	112.117	496	0.6	6.03	4.17 ± 0.05	10.7 ± 0.8	28.9 ± 2.2	69.2 ± 0.8
8. Circle	33.771	112.061	33.772	112.062	538	6.5	6.23	2.61 ± 0.06	18.5 ± 1.4	50.0 ± 3.7	41.9 ± 1.0
9. Charlie	33.774	111.949	33.778	111.931	674	1.2	6.89	1.83 ± 0.03	29.6 ± 2.1	79.9 ± 5.7	26.5 ± 0.5
10. Rock	33.760	111.877	33.762	111.868	771	2.6	7.39	1.29 ± 0.07	45.4 ± 4.0	122.4 ± 10.8	17.5 ± 1.0
11. Cave Creek	33.822	111.860	33.824	111.857	864	1.9	7.92	5.99 ± 0.07	9.2 ± 0.7	24.9 ± 1.9	75.6 ± 0.8
12. Buckhorn	33.772	111.727	33.787	111.760	743	1.5	7.24	2.62 ± 0.04	21.0 ± 1.5	56.7 ± 4.1	36.2 ± 0.5
13. The Rocks	33.736	111.841	33.744	111.835	825	2.2	7.69	1.38 ± 0.03	43.9 ± 3.1	118.4 ± 8.5	17.9 ± 0.4
14. 128th St	33.720	111.806	33.718	111.814	816	1.7	7.64	1.25 ± 0.03	48.2 ± 3.4	130.1 ± 9.3	16.4 ± 0.4
15. 128th St 2	33.716	111.791	33.715	111.798	783	1.7	7.45	1.35 ± 0.03	43.7 ± 3.2	118.1 ± 8.6	18.1 ± 0.5
16. Asher Hills	33.730	111.705	33.737	111.747	671	1.3	6.87	2.63 ± 0.04	19.9 ± 1.4	53.8 ± 3.9	38.3 ± 0.6
17. Gold Cyn	33.368	111.515	33.373	111.498	513	0.6	6.06	3.33 ± 0.05	13.8 ± 1.0	37.3 ± 2.8	54.9 ± 0.8
18. Peralta	33.335	111.430	33.345	111.417	577	2.0	6.36	1.34 ± 0.03	38.7 ± 2.7	104.6 ± 7.3	21.0 ± 0.5

[a] Basin metrics used as input for calculating erosion rates using the CRONUS erosion rate calculator (v 2.2) [61]. [b] Total catchment averaged production rates were calculated using the CRONUS calculator (v 2.2) [61], which includes spallogenic and muogenic production. The reference production rate for sea-level and high latitude is 4.49 atoms g^{-1} yr^{-1} [63]. [c] Normalized with standard 07KNSTD and corrected for process blank. Error propagation was based on Balco et al. [61]. A large value between the internal error and the external error was selected. [d] Timescale of the catchment averaged denudation rate was calculated by dividing the ^{10}Be concentration by the total production rate, which accounts for the duration over which a depth of $z^* = \Lambda/\rho \sim 60$ cm surface in the eroded basin.

Catchments with granitic rocks have higher rates of erosion than catchments that have a mixture of rock types (e.g., metamorphic, basalt, rhyolite, and granitic). This result was verified by a *t*-test comparing natural background sediment yields of granitic versus other rock types; the *t*-test result is statistically significant at $p < 0.05$ (Table 5). This difference is shown graphically in Figure 7. However, there is a problem with this simple statistical test in that rock type and mean slope are very much related. The granitic rock types occur in steeper catchments, while the non-granitic types have lower slopes; the reason for this is due to the geomorphic history of the region and not due to rock type [87].

We confirmed the correlation between rock type and catchment slope by using a *t*-test to compare the mean slope of granitic versus other rock types, where our null hypothesis was that there would be no difference in slopes between different rock types. We rejected this hypothesis of no difference after finding a statistically significant difference for granite (M = 1.76, SD = 0.46) versus other rock type (M = 0.98, SD = 0.6) conditions, t(13) = 2.91, $p < 0.05$ (Table 5). This difference is shown graphically in Figure 7B.

Table 4. Correlation matrix between CADRs and key stock tank catchment variables.

	CADR	Mean Slope	Mean Elevation	Relief	Drainage Area	Drainage Density
CADR	1					
Mean slope	0.75 **	1				
Mean elevation	0.63 **	0.8 **	1			
Relief	0.09	0.2	0.29	1		
Drainage area	–0.25	–0.31	–0.19	0.44	1	
Drainage density	0.34	0.25	0.42	–0.2	–0.49 *	1

Note: $n = 16$, * Significant at $p < 0.1$. ** Significant at $p < 0.05$.

Table 5. Student's *t*-tests results for rock types.

	1. CADR		2. Mean slope	
	Granitic	Non-Granitic	Granitic	Non-Granitic
Mean	88.06	42.13	1.76	0.98
Variance	1567.79	941.61	0.21	0.36
Observations	8	8	8	8
Hypothesized Mean Difference	0		0	
df	13		13	
t Stat	2.59		2.91	
P(T ≤ t) one-tail	0.011		0.006	
t Critical one-tail	1.77		1.77	
P(T ≤ t) two-tail	0.022		0.012	
t Critical two-tail	2.16		2.16	

4.3. Acceleration of Erosion by Different Land Uses

The desert pediments and alluvial fans of the study region (Figures 2 and 3) show a significant sensitivity to soil erosion from an anthropogenic disturbance [33]. Figure 8 takes data presented in Table 6, monitoring soil erosion over two decades, and places them in a ratio over CADR data presented in Table 3. Note that the conventions for units of erosion differ in the cosmogenic nuclide CADR literature and soil erosion scholarship (Table 1). CADRs are presented in terms of meters per million years, and Table 3 makes the conversion to the specific sediment yield more commonly used in soil erosion studies (see Table 1 (1-3)).

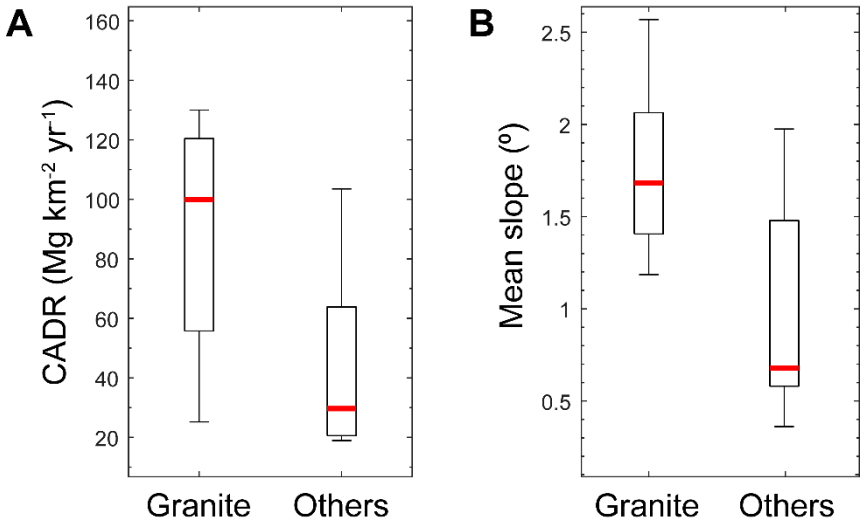

Figure 7. Box and whisker plots comparing granite and other rock types for CADR and mean slope. (**A**) Box and whisker plots to compare the CADR of granite and other rock types. (**B**) Box and whisker plots to compare the mean slope of granite and other rock types. Boxes range from the 25th to 75th percentiles. Whiskers represent the data range. Red lines are medians.

The last two columns in Table 6 are data used to construct Figure 8. The labels in Table 6 of "minimum acceleration" and "maximum acceleration" relate to uncertainty over the source of silts and clays measured by Jeong and Dorn [33], who could not determine whether these came from weathering of rocks in the catchment or were blown in as desert dust. Thus, the "maximum" assumes that all of the accumulated sediment derived from erosion of catchment soils, whereas the "minimum" assumes that only the fine sand and larger size fractions are due to catchment erosion. Thus, the two graphs in Figure 8 depend on the assumption that the fines (silt and clay) that were deposited in the stock ponds were either all blown in or were sourced by weathering in the catchment.

The order of land use presented in Figure 8 reflects the typical change over time as the Phoenix metropolitan region expanded. The first period always involves cattle grazing. We were surprised that not all catchments experienced an acceleration above natural background rates from grazing. For those catchments experiencing an increase in erosion rate above the natural background due to grazing, the highest acceleration was 2.3–2.6 times.

Several catchments were burned by wildfire (Table 6). The designation "Fire1" in Table 6 is the period immediately after the fire, and Fire2 reflects a lower rate of erosion as vegetation grew back; Table 6 details the time periods of post-fire measurements. Immediately after the wildfire, sediment yields increased up to 9.7–10.4 times higher with a median increase of 2.9–3.2 times. After some vegetation grew back, the acceleration was less-up to 4.2–4.5 times higher with a median increase of 1.3–1.4 times.

Construction of subdivisions, commercial property, and infrastructure such as water tanks involves the exposure of bare ground. The "construction" category in Figure 8 lumps all these together. Construction increased sediment yields up to 5.0–5.6 times higher with a median increase of 2.9–3.3 times.

We continued our monitoring after construction and after the sealing of surfaces with concrete, asphalt, buildings, and landscaping. The sealing of urban surfaces led to one-tenth to one-half of sediment yields compared with natural background rates.

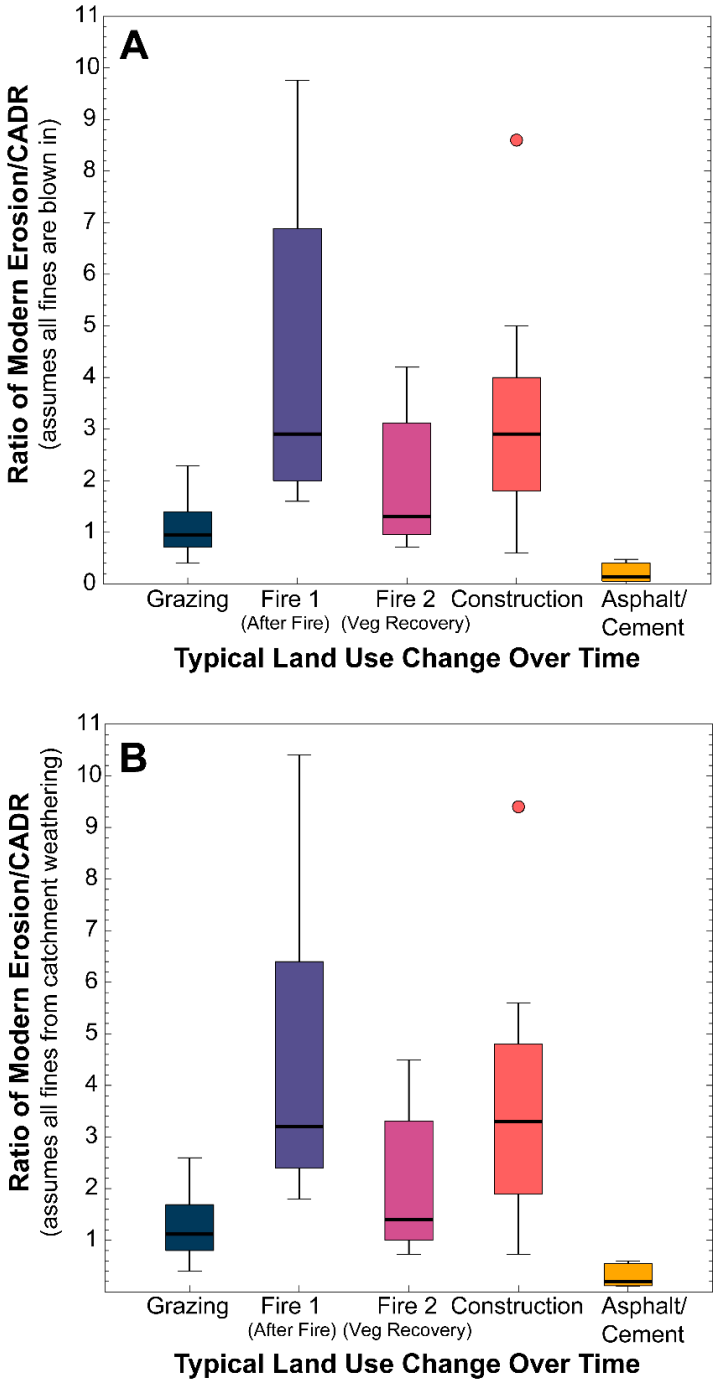

Figure 8. A comparison of the acceleration of specific sediment yields above natural backgrounds by different land uses in the Phoenix metropolitan area. The ratio was constructed from: (**A**) the minimum area-specific sediment yield calculated with the assumption that all fines are blown in divided by the CADR (i.e., the minimum acceleration in Table 6); and (**B**) the maximum area-specific sediment yield calculated with the assumption that all fines are from catchment weathering divided by the CADR (i.e., the maximum acceleration in Table 6).

Table 6. Data on the stock tank catchments needed to calculate soil erosion, along with other watershed characteristics used in modeling soil erosion for the Phoenix metropolitan region (PMR). The last two columns (maximum and minimum acceleration) are a ratio of modern SSY to background SSY (from Table 3).

Sample ID	Time Period	Field Description of Dominant Land Use [a]	Land Use [b]	Different Rock Types	MAP (mm) (I30) (mm)		Ad (km^2)	At (m^2)	Modern SSY [c] $\pm 1\sigma$ (Mg km^{-2} yr^{-1})	Modern SSY [d] $\pm 1\sigma$ (Mg km^{-2} yr^{-1})	Background SSY $\pm 1\sigma$ (Mg km^{-2} yr^{-1})	Minimum Acceleration	Maximum Acceleration
					P1	P2							
1. Cigar	1990–2004	grazing	C	metamorphic, basalt, granite	207(20.9)	170(15.4)	2.6	6000	77.3 ± 3.8	89.2 ± 9.7	19.3 ± 1.5	4.0	4.6
	2005–2009	grazing and off-road vehicle use	C						89.6 ± 3.2	102.4 ± 9.8		4.6	5.3
2. Saguaro	1990–2004	grazing	G	metamorphic, basalt, granite	222(25.1)	181(14.1)	1.4	5800	41.4 ± 3.2	48.7 ± 7.6	32.7 ± 2.4	1.3	1.5
	2005–2009	grazing & pipeline construction	C						126.7 ± 4.6	143.2 ± 26.0		3.9	4.4
3. Cline	1989–1995	Some construction	C	metamorphic, basalt, granite	222(25.1)	181(14.1)	1.5	9500	44.4 ± 5.4	52.0 ± 6.9	18.7 ± 1.5	2.4	2.8
	1996–2003	commercial construction	C						92.7 ± 3.1	103.7 ± 6.4		5.0	5.6
	2003–2004	subdivision construction	C						160 ± 10.9	174.7 ± 25.4		8.6	9.4
4. Anthem	1989–1992	grazing	G	metavolcanic	222(25.1)	181(14.1)	0.88	3000	121.4 ± 15.8	136.7 ± 14.6	52.2 ± 3.8	2.3	2.6
	1993–1997	after wildfire	F1						309.3 ± 27.4	334.0 ± 25.4		5.9	6.4
5. Anthem 2	1989–1992	grazing	G	metavolcanic	222(25.1)	181(14.1)	0.58	2700	67.1 ± 2.9	77.5 ± 7.1	73.0 ± 5.2	0.9	1.1
	1993–1995	after wildfire period 1	F1						254 ± 24.6	276.7 ± 45.8		3.5	3.8
	1996–1998	after wildfire period 2	F2						308.6 ± 58.4	330.9 ± 32.8		4.2	4.5
	1999–2002	after wildfire period 3	F2						146 ± 20.0	156.2 ± 14.9		2.0	2.1
	2002	housing	C						230.1 ± 12.8	255.7 ± 41.4		3.2	3.5
	2006–2008	after subdivision built	S						12.9 ± 0.6	15.9 ± 4.0		0.2	0.2
6. Pepe	1989–2008	grazing and ongoing house construction	G	metamorphic, basalt, granite	222(22.8)	181(11.5)	0.99	3300	31.3 ± 3.7	38.4 ± 10.0	22.6 ± 1.7	1.4	1.7
7. Bronco	1989–1998	grazing	G	metamorphic, basalt, granite	222(22.8)	181(11.5)	0.45	4100	37.4 ± 5.4	43.7 ± 8.0	28.9 ± 2.2	1.3	1.5
	1999–2003	road construction	C						112.5 ± 11.2	137.4 ± 32.4		3.9	4.8
8. Circle	1990–2010	grazing	G	metamorphic	222(22.8)	181(11.5)	0.6	5000	42.5 ± 4.1	51.0 ± 13.7	50.0 ± 3.7	0.9	1.0
	2010–2013	road construction	C						112.3 ± 4.9	128.5 ± 31.1		2.2	2.6
9. Charlie	1989–2004	house construction	C	granitic	276(40.4)	237(28.0)	0.91	10500	235.6 ± 11.1	264.3 ± 49.1	79.9 ± 5.7	2.9	3.3
10. Rock	1989–1992	grazing	G	granitic	276(40.4)	237(28.0)	0.54	2800	45.7 ± 3.5	53.6 ± 8.8	122.4 ± 10.8	0.4	0.4
	1992–1997	after wildfire period 1	F1						199 ± 14.3	224.0 ± 25.3		1.6	1.8
	1998–2003	after wildfire period 2	F2						159.3 ± 24.9	175.7 ± 11.7		1.3	1.4
	2004–2009	after wildfire period 3	F2						85 ± 17.2	90.9 ± 9.3		0.7	0.7

Table 6. *Cont.*

Sample ID	Time Period	Field Description of Dominant Land Use [a]	Land Use [b]	Different Rock Types	MAP (mm) (I30) (mm) P1	MAP (mm) (I30) (mm) P2	Ad (km^2)	At (m^2)	Modern SSY [c] $\pm 1\sigma$ (Mg km^{-2} yr^{-1})	Modern SSY [d] $\pm 1\sigma$ (Mg km^{-2} yr^{-1})	Background SSY $\pm 1\sigma$ (Mg km^{-2} yr^{-1})	Minimum Acceleration	Maximum Acceleration
11. Cave Creek	1989–1992	grazing	G	granitic	276(15.4)	237(22.9)	0.19	1200	89.1 ± 10.8	102.2 ± 15.4	24.9 ± 1.9	3.6	4.1
	1992–1999	after wildfire	F1						242.6 ± 39.8	258.5 ± 18.0		9.7	10.4
	2000–2003	house construction	C						114.3 ± 8.7	128.8 ± 23.6		4.6	5.2
	2010–2013	after subdivision built	S						12.7 ± 0.5	14.7 ± 3.0		0.5	0.6
12. Buckhorn	1989–1999	grazing	C	granitic	305(40.4)	260(28.0)	4.4	4100	91.6 ± 5.4	106.2 ± 17.1	56.7 ± 4.1	1.6	1.9
	2000–2002	house construction	C						115.7 ± 15.2	133.4 ± 17.4		2.0	2.4
13. The Rocks	1989–1996	house construction	C	granitic	310(40.4)	248(28.0)	2.36	6500	212.9 ± 28.0	227.6 ± 25.7	118.4 ± 8.5	1.8	1.9
	1996–1998	after subdivision built	S						15.8 ± 1.0	17.8 ± 4.6		0.1	0.2
14. 128th St	1989–1994	grazing	G	granitic	310(40.4)	248(28.0)	0.85	7000	94.7 ± 13.6	110.3 ± 27.1	130.1 ± 9.3	0.7	0.8
	1995–2000	after wildfire	F1						302.3 ± 10.8	342.0 ± 40.4		2.3	2.6
	2001–2008	road construction	C						141.3 ± 7.4	159.9 ± 29.4		1.1	1.2
15. 128th St 2	1989–1994	grazing	G	granitic	310(40.4)	248(28.0)	0.31	2200	94.5 ± 12.4	109.5 ± 45.9	118.1 ± 8.6	0.8	0.9
	1995–2000	after wildfire	F1						250 ± 15.9	278.7 ± 94.4		2.1	2.4
	2001–2008	road construction	F2						135.7 ± 12.2	149.1 ± 48.4		1.1	1.3
16. AsherHills	1989–2001	grazing	C	granitic	310(17.5)	248(18.4)	2.1	9800	125.9 ± 11.6	140.5 ± 27.6	53.8 ± 3.9	2.3	2.6
	2002–2007	house construction	C						182.6 ± 7.9	199.1 ± 15.0		3.4	3.7
17. Gold Cyn	1989–2009	cattle grazing & house construction	C	ignimbrite, granitic	254(23.2)	209(17.9)	5.1	18000	45.3 ± 2.5	57.3 ± 13.1	37.3 ± 2.8	1.2	1.5
18. Peralta	1989–2000	grazing	G	ignimbrite, granitic, breccia	254(23.2)	209(17.9)	0.78	2800	44.7 ± 3.0	52.2 ± 3.8	104.6 ± 7.3	0.4	0.5
	2001–2005	subdivision construction	C						61.5 ± 3.9	77.4 ± 6.8		0.6	0.7
	2006–2009	after subdivision built	S						6.2 ± 0.4	8.7 ± 2.8		0.1	0.1

Note: Abbreviations are as follows: MAP, mean annual precipitation during the 10-year period of study; P1, Period 1 (1989–1999); P2, Period 2 (2000–2009); I30, the total amount of rainfall that exceeded 10 mm for 30 min; Ad, drainage area; At, tank area; SSY, area-specific sediment yield. [a] Field description of the dominant land use reported by Jeong and Dorn [33]. [b] Dominant land use classified by this study. G, grazing; F1, immediately after a wildfire (typically 3–5 years); F2, after the F1 time period where some revegetation has occurred; C, construction in stock pond catchments; S, sealing by impervious materials. Land use land cover (LULC) was mainly classified using a LULC map supplemented by field observations and Google Earth satellite imagery. For example, some construction areas we monitored from the field were not classified in the LULC map. Then, using the Google Earth satellite imagery, we manually calculated the area of exposed bare ground due to construction activities when we could observe clear construction activities from the satellite imagery. [c] Minimum SSY in the unit of Mg (metric ton) km^{-2} yr^{-1}, which was calculated assuming that all fines are blown in [33]. [d] Maximum SSY in the unit of Mg (metric ton) km^{-2} yr^{-1}, which was calculated assuming that all fines are from catchment weathering [33].

5. Discussion

5.1. Soil Erosion in Arid Lands

Borrelli et al. [8] conducted an exhaustive and systematic review of soil erosion modeling, indicating that the greatest number of studies exist in temperate and Mediterranean zones with far fewer studies in arid lands. Perhaps the most detailed compilation of soil erosion in warm deserts comes from Vanmaercke et al. [88] who compiled Köppen-Geiger BWh data for Africa. More recent research by Vaezi et al. [40] revealed that slope steepness, vegetation cover, and soil erodibility factor have a statistically significant relationship with sediment yield in the northwest of Iran.

Figure 9 presents a plot of available data on BWh sediment yield, compiled by Jeong and Dorn [33], where arid data plot between African [88] and European [89] compilations for modern sediment yields. We also plot our CADR data for the 18 Phoenix-region watersheds in Figure 9, along with previously compiled [90] CADR data for arid regions-both tectonically active and tectonically inactive. Note that CADR data follow the same basic trend of increased area-specific sediment yield in smaller watersheds, but the relationship between CADR-SSY and drainage area is not statistically significant. We note that the median SSY for all CADR data is 71 Mg Km^{-2} yr^{-1}, and this is about two-thirds of the modern median for the SSY at 110 Mg Km^{-2} yr^{-1} for BWh climates.

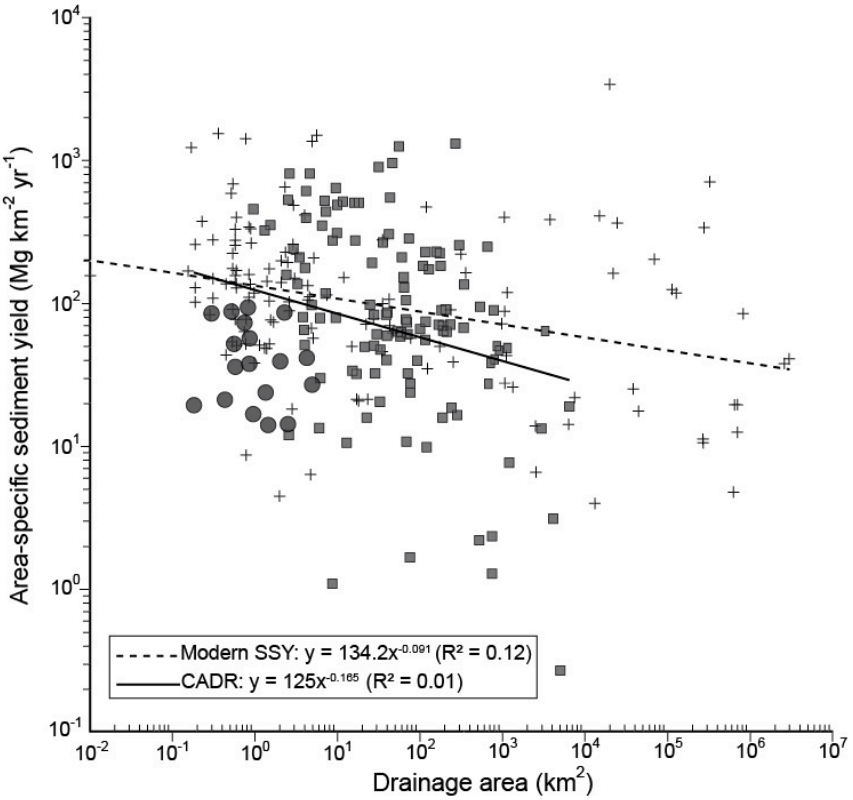

Figure 9. Comparison of the modern area-specific sediment yield in BWh climates (+ symbol) compiled by Jeong and Dorn [33] with pre-anthropogenic background sediment yields obtained by ^{10}Be CADR measurements in this study (solid circles) and those compiled previously [90] for arid regions (solid squares).

Figure 10 compares our CADR data from the Sonoran Desert with other CADRs from arid and semi-arid watersheds compiled by Harel et al. [90]. We reclassified the global ^{10}Be denudation rate compilation [90] into four different groups based on climate and seismic activity, and our Sonoran Desert background soil erosion data (Table 3) are similar to other tectonically inactive and arid watersheds.

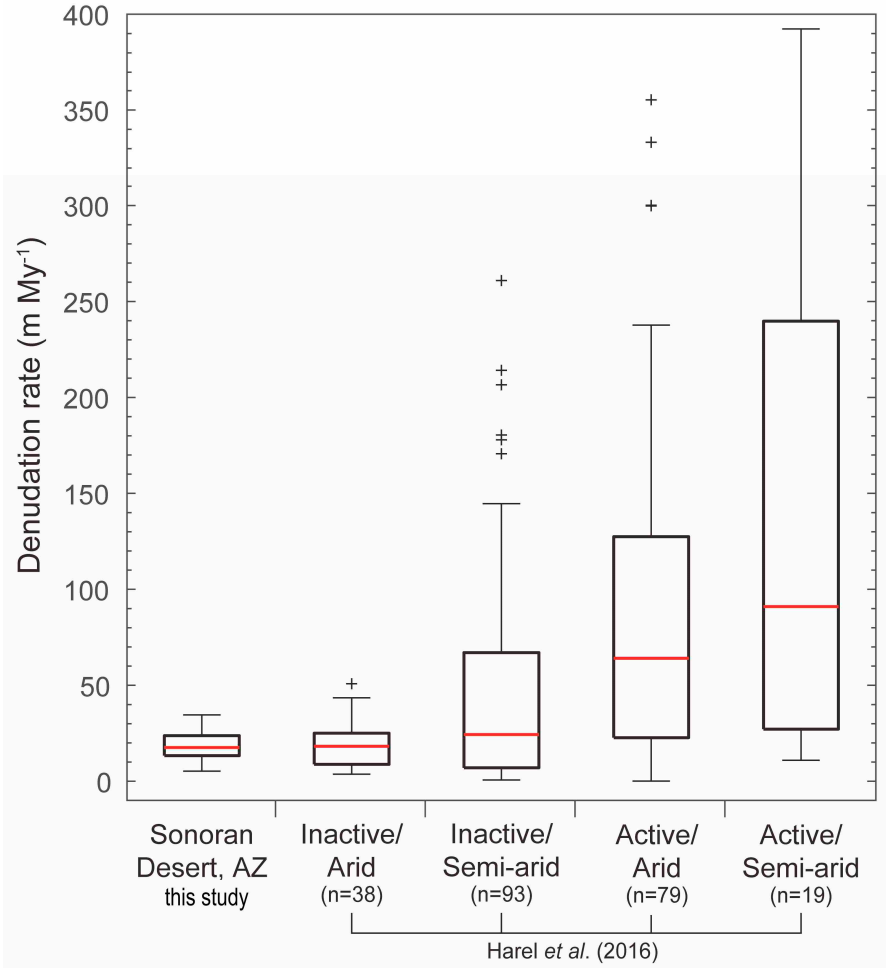

Figure 10. Box plots comparing the ^{10}Be denudation rates we observed in the tectonically inactive Sonoran Desert with a global-scale ^{10}Be denudation analysis [90]. Inactive/arid regions have a seismicity < 2 categorized by Harel et al. [90] and a mean annual precipitation (MAP) of <250 mm. Inactive/semiarid regions also have a seismicity < 2 categorized by Harel et al. [90] but a mean annual precipitation (MAP) of greater than 250 mm but less than 500 mm. Active/arid regions have a seismicity > 2 categorized by Harel et al. [90] and a mean annual precipitation (MAP) of <250 mm. Active/semiarid regions also have a seismicity > 2 categorized by Harel et al. [90] but a mean annual precipitation (MAP) of >250 mm but <500 mm.

5.2. Grazing's Acceleration of Erosion

Grazing has long been recognized as an important factor influencing soil erosion in arid lands [40,91–96]. Fourteen of the 18 Phoenix-area watersheds were monitored during the period when grazing was the predominant land use (Table 6). When we compared natural CADR erosion rates (Table 3) to the period of grazing in the same Sonoran Desert watershed, 6 of the 14 drainage basins did not experience an acceleration of erosion from grazing. The eight watersheds that did experience enhanced erosion compared with the natural background CADR had a minimum acceleration ranging from 1.3x to 4.0x.

In order to explain the unexpected finding of no acceleration in several of the watersheds, we can rule out a prehistoric anthropogenic effect, because the timescales of ^{10}Be CADR results range from 16.4 ka and 101 ka (Table 3). This means that the analyzed quartz particles were exposed to cosmic ranges during the last glacial cycle. Although early humans arrived in the New World at the end of the Pleistocene [97], their effect on erosion would likely have been minimal because of the low population density in this region during the late Pleistocene and Holocene [98].

Another possible explanation as to why grazing did not accelerate erosion above natural backgrounds in six of the watersheds could be due to higher erosion rates in previous wetter climates [99,100] in the 16.4 ka to 101 ka timescale of ^{10}Be exposure (Table 3). Yet another possible explanation would be differences in grazing histories between basins, in that it is possible that the six basins not experiencing an acceleration of erosion from grazing might have had minimal grazing during the time period of monitoring; unfortunately, different grazing histories is a possibility that cannot be evaluated because the only grazing record for the watersheds consists of a permit to graze cattle and not the number of cattle actually on the range in any given year.

5.3. Wildfire's Acceleration of Erosion

Wildfire is widely recognized as an agent that accelerates erosion of soils [7,34,41,101,102]. This is true even in arid regions [103]. Wildfires occurred in 6 of the 18 studied watersheds after monitoring had started. That wildfires took place in one-third of the studied basins is a reflection of the encroachment of the urban boundary and the poor behavior of individuals on these lands, such as lighting cigarettes and letting off-road vehicles stand on tall dry grass.

Erosion after the wildfires was monitored immediately after the fire. Then, for watersheds that did not experience construction from urbanization, we continued to monitor erosion as the vegetation density gradually increased over time. Sediment yields immediately after a fire had median acceleration of 4.2–4.5x, with some watersheds accelerating at rates 10x above the natural background. Then, after a decade of revegetation, the median acceleration dropped to 1.3–1.4x the natural background erosion rates.

Our findings on the acceleration of erosion from wildfire detailed in Table 6 are the first known observations of how much wildfire can accelerate soil erosion in an arid region. Since wildfire did not occur naturally in the Sonoran Desert prior to the invasion of European grasses [50], we are confident that the CADR signal for natural erosion did not include wildfire. The lack of European grasses meant that we could also rule out prehistoric enhancements of erosion rates due to wildfire; our confidence in this interpretation is bolstered by previous observations that the Aboriginal Australian's use of fire was not sufficiently intense or long lasting to alter CADR erosion rates [104].

5.4. Urbanization's Acceleration of Erosion

Although the impact of urbanization processes on soil erosion had been studied previously (e.g., [105,106]), Russell et al. [22] produced the first comprehensive analysis of urbanization's impact on sediment yields. Only 3 of the 18 studied Phoenix-region watersheds did not experience construction activities leading to houses, commercial properties, or other infrastructure such as water tanks. Since our watersheds lacked any gullying, with the largest rills reaching 5 cm in depth, we interpret the impact of construction over the natural background to be the result of exposing bare ground to rainsplash and overland flow. The median acceleration of 2.9–3.3x with the higher end of acceleration being 5.0–5.6x is the first observation of its kind on just how much urbanization can increase soil erosion rates in arid settings. In addition, we obtained the first confirmation that sealing of urban surfaces with asphalt, concrete, buildings, and associated landscaping greatly reduces erosion well below natural rates of erosion-roughly 1/10 to 1/2 CADR measurements.

Some might think of the arid region as already having an abundance of bare ground exposure, and this is true. Jeong and Dorn [33] used historic photography to estimate the vegetation cover of these watersheds during periods of grazing, and coverage ranged from 4% to 37%. Our field observations of what happens during rain events in a grazed area as opposed to bare-ground are fully consistent with Cerdà [107], who showed that surface rock fragments slow down runoff to raise infiltration rates and decrease erosion rates. Construction removes the natural cover of cobbles that often form as a lag in the Sonoran Desert [108], which could be part of the explanation of urbanization's acceleration of soil erosion.

The stakes associated with urbanization-enhanced soil erosion tend to be spatially variable, as is the case for all soil erosion [19,31,109]. For example, the effects of urban soil erosion in the Phoenix area are relatively minor—impacting such issues as reservoirs [55], water quality [110], and health effects from heavy metals [111]. In other cities, soil erosion can impact the urban poor in a variety of ways, including a negative health impact [112] and water quality [113]. Some value urban soils as vital for urban agriculture and a pathway towards sustainability [114]. Enhanced urban soil erosion might remove carbon stored in city soils [115,116], or it might end up in a setting where it can be more stable, such as a reservoir [117].

6. Conclusions

The concept of an Anthropocene epoch, starting with the onset of a significant human impact on the Earth, has been debated in soils [118] and geomorphological scholarship [119], with the hypothesis of a "great acceleration" [120] associated with anthropogenic activities. Here, for the first time, we place specific numbers on the acceleration of erosion above natural background rates in the Sonoran Desert of Arizona, United States from grazing, wildfires, and urbanization.

Knowing just how much grazing, wildfire, and urbanization can increase soil erosion above natural rates has implications for the sustainable management of arid-region soils. The accelerated soil erosion by human activities is a major concern for land management with respect to soil degradation (e.g., [11,12,15,19,22,36,121–125]). Through their extensive review of tolerable soil erosion rates for human society, Verheijen et al. [126] concluded that soil functions can generally be maintained as long as soil erosion does not exceed natural erosion rates. Thus, our framework for combining erosion monitoring and CADRs would allow land managers to have a better understanding of the quantitative target rate of erosion that can maintain good ecological status and halt or potentially reverse land degradation [127]. This research illustrates that a quantitative target of a natural background rate of erosion would be particularly useful when planning and managing different land uses such as vineyards [21,26,122,125,128], specific locations impacted by wildfire [33–35], and construction sites [22,24,33].

Author Contributions: Conceptualization, A.J. and R.I.D.; methodology, A.J., R.I.D., Y.-B.S., and B.-Y.Y.; validation and formal analysis, A.J., R.I.D., and Y.-B.S.; investigation, A.J., R.I.D., and Y.-B.S.; data curation, A.J. and R.I.D.; writing—original draft preparation, A.J. and R.I.D.; writing—review and editing, Y.-B.S.; visualization, A.J.; supervision, R.I.D.; project administration, A.J. All authors have read and agreed to the published version of the manuscript.

Funding: This research received no external funding.

Data Availability Statement: The modern sediment yields data are available at https://doi.org/10.1002/ldr.3207, accessed on 8 April 2021. The data presented in this study are available on request from the corresponding author.

Acknowledgments: We thank T. Dunne, M.W. Schmeeckle, I.J. Walker, and K. Seto for suggestions and Arizona State University for support. We also thank S. Alter and S.Y. Cheung for field assistance and H.H. Rhee, P. Khandsuren, and C.-H. Lee for lab assistance.

Conflicts of Interest: The authors declare no conflict of interest.

References

1. Rodrigo-Comino, J.; González, J.M.S. La Edafogeografía: La quinta rama olvidada de la Geografía Física. *Cuad. Geográficos* **2013**, *52*, 6–28.
2. Rodrigo-Comino, J.; Senciales, J.M.; Cerdà, A.; Brevik, E.C. The multidisciplinary origin of soil geography: A review. *Earth Sci. Rev.* **2018**, *177*, 114–123. [CrossRef]
3. Bezak, N.; Mikoš, M.; Borrelli, P.; Alewell, C.; Alvarez, P.; Anache, J.A.A.; Baartman, J.; Ballabio, C.; Biddoccu, M.; Cerdà, A.; et al. Soil erosion modelling: A bibliometric analysis. *Environ. Res.* **2021**, *197*, 111087. [CrossRef] [PubMed]
4. Amundson, R.; Berhe, A.A.; Hopmans, J.W.; Olson, C.; Sztein, A.E.; Sparks, D.L. Soil and human security in the 21st century. *Science* **2015**, *348*, 1261071. [CrossRef] [PubMed]

5. Muñoz-Rojas, M.; Pereira, P.; Brevik, E.C.; Cerdà, A.; Jordán, A. *Chapter 6—Soil Mapping and Processes Models for Sustainable Land Management Applied to Modern Challenges*; Pereira, P., Brevik, E.C., Muñoz-Rojas, M., Miller, B.A.B.T., Eds.; Elsevier: Amsterdam, The Netherlands, 2017; pp. 151–190. ISBN 978-0-12-805200-6.
6. Schwilch, G.; Lemann, T.; Berglund, Ö.; Camarotto, C.; Cerdà, A.; Daliakopoulos, I.N.; Kohnová, S.; Krzeminska, D.; Marañón, T.; Rietra, R.; et al. Assessing Impacts of Soil Management Measures on Ecosystem Services. *Sustainability* **2018**, *10*, 4416. [CrossRef]
7. Rodrigo-Comino, J.; López-Vicente, M.; Kumar, V.; Rodríguez-Seijo, A.; Valkó, O.; Rojas, C.; Pourghasemi, H.R.; Salvati, L.; Bakr, N.; Vaudour, E.; et al. Soil Science Challenges in a New Era: A Transdisciplinary Overview of Relevant Topics. *Air Soil Water Res.* **2020**, *13*, 1178622120977491. [CrossRef]
8. Borrelli, P.; Alewell, C.; Alvarez, P.; Anache, J.A.A.; Baartman, J.; Ballabio, C.; Bezak, N.; Biddoccu, M.; Cerdà, A.; Chalise, D.; et al. Soil erosion modelling: A global review and statistical analysis. *Sci. Total Environ.* **2021**, *780*, 146494. [CrossRef]
9. Pandey, A.; Bishal, K.C.; Kalura, P.; Chowdary, V.M.; Jha, C.S.; Cerdà, A. A Soil Water Assessment Tool (SWAT) Modeling Approach to Prioritize Soil Conservation Management in River Basin Critical Areas Coupled With Future Climate Scenario Analysis. *Air Soil Water Res.* **2021**, *14*, 11786221211021396. [CrossRef]
10. Granger, D.E.; Schaller, M. Cosmogenic Nuclides and Erosion at the Watershed Scale. *Elements* **2014**, *10*, 369–373. [CrossRef]
11. Nyssen, J.; Poesen, J.; Moeyersons, J.; Luyten, E.; Veyret-Picot, M.; Deckers, J.; Haile, M.; Govers, G. Impact of road building on gully erosion risk: A case study from the northern Ethiopian highlands. *Earth Surf. Process. Landf. J. Br. Geomorphol. Res. Gr.* **2002**, *27*, 1267–1283. [CrossRef]
12. Nyssen, J.; Poesen, J.; Moeyersons, J.; Deckers, J.; Haile, M.; Lang, A. Human impact on the environment in the Ethiopian and Eritrean highlands—a state of the art. *Earth Sci. Rev.* **2004**, *64*, 273–320. [CrossRef]
13. Cerdà, A.; Doerr, S.H. Soil wettability, runoff and erodibility of major dry-Mediterranean land use types on calcareous soils. *Hydrol. Process.* **2007**, *21*, 2325–2336. [CrossRef]
14. García-Orenes, F.; Cerdà, A.; Mataix-Solera, J.; Guerrero, C.; Bodí, M.B.; Arcenegui, V.; Zornoza, R.; Sempere, J.G. Effects of agricultural management on surface soil properties and soil–water losses in eastern Spain. *Soil Tillage Res.* **2009**, *106*, 117–123. [CrossRef]
15. Maetens, W.; Vanmaercke, M.; Poesen, J.; Jankauskas, B.; Jankauskiene, G.; Ionita, I. Effects of land use on annual runoff and soil loss in Europe and the Mediterranean: A meta-analysis of plot data. *Prog. Phys. Geogr.* **2012**, *36*, 599–653. [CrossRef]
16. Taye, G.; Poesen, J.; Van Wesemael, B.; Vanmaercke, M.; Teka, D.; Deckers, J.; Goosse, T.; Maetens, W.; Nyssen, J.; Hallet, V.; et al. Effects of land use, slope gradient, and soil and water conservation structures on runoff and soil loss in semi-arid Northern Ethiopia. *Phys. Geogr.* **2013**, *34*, 236–259. [CrossRef]
17. Taye, G.; Vanmaercke, M.; Poesen, J.; Van Wesemael, B.; Tesfaye, S.; Teka, D.; Nyssen, J.; Deckers, J.; Haregeweyn, N. Determining RUSLE P- and C-factors for stone bunds and trenches in rangeland and cropland, North Ethiopia. *Land Degrad. Dev.* **2018**, *29*, 812–824. [CrossRef]
18. Wei, W.; Chen, L.; Zhang, H.; Yang, L.; Yu, Y.; Chen, J. Effects of crop rotation and rainfall on water erosion on a gentle slope in the hilly loess area, China. *CATENA* **2014**, *123*, 205–214. [CrossRef]
19. Vanmaercke, M.; Poesen, J.; Govers, G.; Verstraeten, G. Quantifying human impacts on catchment sediment yield: A continental approach. *Glob. Planet. Chang.* **2015**, *130*, 22–36. [CrossRef]
20. Vanmaercke, M.; Panagos, P.; Vanwalleghem, T.; Hayas, A.; Foerster, S.; Borrelli, P.; Rossi, M.; Torri, D.; Casali, J.; Borselli, L.; et al. Measuring, modelling and managing gully erosion at large scales: A state of the art. *Earth Sci. Rev.* **2021**, *218*, 103637. [CrossRef]
21. Rodrigo-Comino, J.; Senciales, J.M.; Ramos, M.C.; Martínez-Casasnovas, J.A.; Lasanta, T.; Brevik, E.C.; Ries, J.B.; Ruiz Sinoga, J.D. Understanding soil erosion processes in Mediterranean sloping vineyards (Montes de Málaga, Spain). *Geoderma* **2017**, *296*, 47–59. [CrossRef]
22. Russell, K.L.; Vietz, G.J.; Fletcher, T.D. Global sediment yields from urban and urbanizing watersheds. *Earth Sci. Rev.* **2017**, *168*, 73–80. [CrossRef]
23. Russell, K.L.; Vietz, G.J.; Fletcher, T.D. A suburban sediment budget: Coarse-grained sediment flux through hillslopes, stormwater systems and streams. *Earth Surf. Process. Landf.* **2019**, *44*, 2600–2614. [CrossRef]
24. Russell, K. Potential sediment supply fluxes associated with greenfield residential construction. *Anthropocene* **2021**, *35*, 100300. [CrossRef]
25. Zhang, Y.; Bi, Z.; Zhang, X.; Yu, Y. Influence of Landscape Pattern Changes on Runoff and Sediment in the Dali River Watershed on the Loess Plateau of China. *Land* **2019**, *8*, 180. [CrossRef]
26. Barrena-González, J.; Rodrigo-Comino, J.; Gyasi-Agyei, Y.; Pulido Fernández, M.; Cerdà, A. Applying the RUSLE and ISUM in the Tierra de Barros Vineyards (Extremadura, Spain) to Estimate Soil Mobilisation Rates. *Land* **2020**, *9*, 93. [CrossRef]
27. Heimsath, A.M.; Dietrich, W.E.; Nishiizumi, K.; Finkel, R.C. The soil production function and landscape equilibrium. *Nature* **1997**, *388*, 358–361. [CrossRef]
28. Kelly, M.A.; Lowell, T.V.; Hall, B.L.; Schaefer, J.M.; Finkel, R.C.; Goehring, B.M.; Alley, R.B.; Denton, G.H. A 10Be chronology of lateglacial and Holocene mountain glaciation in the Scoresby Sund region, east Greenland: Implications for seasonality during lateglacial time. *Quat. Sci. Rev.* **2008**, *27*, 2273–2282. [CrossRef]
29. Montgomery, D.R. Soil erosion and agricultural sustainability. *Proc. Natl. Acad. Sci. USA* **2007**, *104*, 13268–13272. [CrossRef]
30. Montgomery, D.R. *Dirt: The Erosion of Civilizations*; University of California Press: Berkeley, CA, USA, 2012; ISBN 0520272900.
31. Poesen, J. Soil erosion in the Anthropocene: Research needs. *Earth Surf. Process. Landf.* **2018**, *43*, 64–84. [CrossRef]

32. Jeong, A.; Cheung, S.Y.; Walker, I.J.; Dorn, R.I. Urban Geomorphology of an Arid City: Case Study of Phoenix, Arizona. In *Urban Geomorphology Landforms and Processes in Cities*; Thornbush, M.J., Allen, C.D., Eds.; Elsevier: Oxford, UK, 2018; pp. 177–204. ISBN 978-0-12-811951-8.
33. Jeong, A.; Dorn, R.I. Soil erosion from urbanization processes in the Sonoran Desert, Arizona, USA. *Land Degrad. Dev.* **2019**, *30*, 226–238. [CrossRef]
34. Cerdá, A.; Doerr, S.H. Influence of vegetation recovery on soil hydrology and erodibility following fire: An 11-year investigation. *Int. J. Wildl. Fire* **2005**, *14*, 423–437. [CrossRef]
35. Cerdà, A.; Doerr, S.H. The effect of ash and needle cover on surface runoff and erosion in the immediate post-fire period. *CATENA* **2008**, *74*, 256–263. [CrossRef]
36. Mekuria, W.; Veldkamp, E.; Haile, M.; Nyssen, J.; Muys, B.; Gebrehiwot, K. Effectiveness of exclosures to restore degraded soils as a result of overgrazing in Tigray, Ethiopia. *J. Arid. Environ.* **2007**, *69*, 270–284. [CrossRef]
37. Nearing, M.A.; Xie, Y.; Liu, B.; Ye, Y. Natural and anthropogenic rates of soil erosion. *Int. Soil Water Conserv. Res.* **2017**, *5*, 77–84. [CrossRef]
38. Western Regional Climate Center. Cooperative Climatological Data Summaries. Available online: https://wrcc.dri.edu/cgi-bin/cliMAIN.pl?az6486 (accessed on 22 July 2021).
39. Climate Office of Arizona. Climate of Phoenix Summary. Available online: https://azclimate.asu.edu/climate/climate-of-phoenix-summary/ (accessed on 22 January 2021).
40. Vaezi, A.R.; Abbasi, M.; Keesstra, S.; Cerdà, A. Assessment of soil particle erodibility and sediment trapping using check dams in small semi-arid catchments. *CATENA* **2017**, *157*, 227–240. [CrossRef]
41. Mohammed, S.; Abdo, H.G.; Szabo, S.; Pham, Q.B.; Holb, I.J.; Linh, N.T.; Anh, D.T.; Alsafadi, K.; Mokhtar, A.; Kbibo, I.; et al. Estimating Human Impacts on Soil Erosion Considering Different Hillslope Inclinations and Land Uses in the Coastal Region of Syria. *Water* **2020**, *12*, 2786. [CrossRef]
42. Allen, C.D. Micrometeorology of a Smooth and Rugose Biological Soil Crust near Coon Bluff, Arizona. *J. Ariz. Nev. Acad. Sci.* **2005**, *38*, 21–28. [CrossRef]
43. Allen, C.D. Biogeomorphology and biological soil crusts: A symbiotic research relationship. *Géomorphol. Relief Process. Environ.* **2010**, *16*, 347–358.
44. Nagy, M.L.; Pérez, A.; Garcia-Pichel, F. The prokaryotic diversity of biological soil crusts in the Sonoran Desert (Organ Pipe Cactus National Monument, AZ). *FEMS Microbiol. Ecol.* **2005**, *54*, 233–245. [CrossRef]
45. Fernández-Raga, M.; Palencia, C.; Keesstra, S.; Jordán, A.; Fraile, R.; Angulo-Martínez, M.; Cerdà, A. Splash erosion: A review with unanswered questions. *Earth Sci. Rev.* **2017**, *171*, 463–477. [CrossRef]
46. Vanmaercke, M.; Makanzu Imwangana, F.; Cogels, S.; Dewitte, O.; Trefon, T.; Bielders, C.; Poesen, J.; Wazi Nandefo, R.; Mbalanda Lawunda, W. Prevention and Mitigation of Urban Gullies: Lessons learned from Failures and Successes. In Proceedings of the EGU General Assembly Conference Abstracts, Vienna, Austria, 4–13 April 2018; p. 7126.
47. Bartley, R.; Poesen, J.; Wilkinson, S.; Vanmaercke, M. A review of the magnitude and response times for sediment yield reductions following the rehabilitation of gullied landscapes. *Earth Surf. Process. Landf.* **2020**, *45*, 3250–3279. [CrossRef]
48. Rodrigo-Comino, J.; Martínez-Hernández, C.; Iserloh, T.; Cerdà, A. Contrasted Impact of Land Abandonment on Soil Erosion in Mediterranean Agriculture Fields. *Pedosphere* **2018**, *28*, 617–631. [CrossRef]
49. Esmali Ouri, A.; Golshan, M.; Janizadeh, S.; Cerdà, A.; Melesse, A.M. Soil Erosion Susceptibility Mapping in Kozetopraghi Catchment, Iran: A Mixed Approach Using Rainfall Simulator and Data Mining Techniques. *Land* **2020**, *9*, 368. [CrossRef]
50. Humphrey, R.R. The role of fire in the desert and desert grassland areas of Arizona. In Proceedings of the Tall Timbers Fire Ecology Conference, Tallahassee, FL, USA, 14–15 March 1963; Volume 2, pp. 45–62.
51. Brooks, M.L. Plant invasions and fire regimes. In *General Technical Report RMRS-GTR-42*; US Forest Service: Ogden, UT, USA, 2008; Volume 6, pp. 33–45.
52. D'Antonio, C.M.; Vitousek, P.M. Biological Invasions by Exotic Grasses, the Grass/Fire Cycle, and Global Change. *Annu. Rev. Ecol. Syst.* **1992**, *23*, 63–87. [CrossRef]
53. Brooks, M.L.; Chambers, J.C. Resistance to Invasion and Resilience to Fire in Desert Shrublands of North America. *Rangel. Ecol. Manag.* **2011**, *64*, 431–438. [CrossRef]
54. Gober, P.; Trapido-Lurie, B. *Metropolitan Phoenix: Place Making and Community Building in the Desert*; University of Pennsylvania Press: Philadelphia, PA, USA, 2006; ISBN 0812219279.
55. Jeong, A. Sediment accumulation expectations for growing desert cities: A realistic desired outcome to be used in constructing appropriately sized sediment storage of flood control structures. *Environ. Res. Lett.* **2019**, *14*, 125005. [CrossRef]
56. Foster, M.A.; Anderson, R.S. Assessing the effect of a major storm on 10BE concentrations and inferred basin-averaged denudation rates. *Quat. Geochronol.* **2016**, *34*, 58–68. [CrossRef]
57. Seong, Y.B.; Larson, P.H.; Dorn, R.I.; Yu, B.Y. Evaluating process domains in small arid granitic watersheds: Case study of Pima Wash, South Mountains, Sonoran Desert, USA. *Geomorphology* **2016**, *255*, 108–124. [CrossRef]
58. Nishiizumi, K.; Kohl, C.P.; Shoemaker, E.M.; Arnold, J.R.; Klein, J.; Fink, D.; Middleton, R. In situ10Be-26Al exposure ages at Meteor Crater, Arizona. *Geochim. Cosmochim. Acta* **1991**, *55*, 2699–2703. [CrossRef]
59. Jeong, A.; Lee, J.I.; Seong, Y.B.; Balco, G.; Yoo, K.-C.; Yoon, H.I.; Domack, E.; Rhee, H.H.; Yu, B.Y. Late Quaternary deglacial history across the Larsen B embayment, Antarctica. *Quat. Sci. Rev.* **2018**, *189*, 134–148. [CrossRef]

60. Nishiizumi, K.; Imamura, M.; Caffee, M.W.; Southon, J.R.; Finkel, R.C.; McAninch, J. Absolute calibration of 10Be AMS standards. *Nucl. Instrum. Methods Phys. Res. Sect. B Beam Interact. Mater. At.* **2007**, *258*, 403–413. [CrossRef]
61. Balco, G.; Stone, J.O.; Lifton, N.A.; Dunai, T.J. A complete and easily accessible means of calculating surface exposure ages or erosion rates from 10Be and 26Al measurements. *Quat. Geochronol.* **2008**, *3*, 174–195. [CrossRef]
62. Lal, D. Cosmic ray labeling of erosion surfaces: In situ nuclide production rates and erosion models. *Earth Planet. Sci. Lett.* **1991**, *104*, 424–439. [CrossRef]
63. Stone, J.O. Air pressure and cosmogenic isotope production. *J. Geophys. Res. Solid Earth* **2000**, *105*, 23753–23759. [CrossRef]
64. Heisinger, B.; Lal, D.; Jull, A.J.T.; Kubik, P.; Ivy-Ochs, S.; Neumaier, S.; Knie, K.; Lazarev, V.; Nolte, E. Production of selected cosmogenic radionuclides by muons: 1. Fast muons. *Earth Planet. Sci. Lett.* **2002**, *200*, 345–355. [CrossRef]
65. Heisinger, B.; Lal, D.; Jull, A.J.T.; Kubik, P.; Ivy-Ochs, S.; Knie, K.; Nolte, E. Production of selected cosmogenic radionuclides by muons: 2. Capture of negative muons. *Earth Planet. Sci. Lett.* **2002**, *200*, 357–369. [CrossRef]
66. Polyakov, V.O.; Nearing, M.A.; Nichols, M.H.; Scott, R.L.; Stone, J.J.; McClaran, M.P. Long-term runoff and sediment yields from small semiarid watersheds in southern Arizona. *Water Resour. Res.* **2010**, *46*, W09512. [CrossRef]
67. Leopold, L.B. *Hydrology for Urban Land Planning: A Guidebook on the Hydrologic Effects of Urban Land Use*; US Department of the Interior, Geological Survey: Washington, DC, USA, 1968; Volume 554.
68. Zhang, W.; Huang, B. Soil erosion evaluation in a rapidly urbanizing city (Shenzhen, China) and implementation of spatial land-use optimization. *Environ. Sci. Pollut. Res.* **2015**, *22*, 4475–4490. [CrossRef]
69. Li, J.; Deng, J.; Gu, Q.; Wang, K.; Ye, F.; Xu, Z.; Jin, S. The accelerated urbanization process: A threat to soil resources in eastern China. *Sustainability* **2015**, *7*, 7137–7155. [CrossRef]
70. Nearing, M.A.; Jetten, V.; Baffaut, C.; Cerdan, O.; Couturier, A.; Hernandez, M.; Le Bissonnais, Y.; Nichols, M.H.; Nunes, J.P.; Renschler, C.S. Modeling response of soil erosion and runoff to changes in precipitation and cover. *Catena* **2005**, *61*, 131–154. [CrossRef]
71. Li, P.; Mu, X.; Holden, J.; Wu, Y.; Irvine, B.; Wang, F.; Gao, P.; Zhao, G.; Sun, W. Comparison of soil erosion models used to study the Chinese Loess Plateau. *Earth Sci. Rev.* **2017**, *170*, 17–30. [CrossRef]
72. Schaller, M.; Von Blanckenburg, F.; Hovius, N.; Kubik, P.W. Large-scale erosion rates from in situ-produced cosmogenic nuclides in European river sediments. *Earth Planet. Sci. Lett.* **2001**, *188*, 441–458. [CrossRef]
73. Bierman, P.R.; Reuter, J.M.; Pavich, M.; Gellis, A.C.; Caffee, M.W.; Larsen, J. Using cosmogenic nuclides to contrast rates of erosion and sediment yield in a semi-arid, arroyo-dominated landscape, Rio Puerco Basin, New Mexico. *Earth Surf. Process. Landf. J. Br. Geomorphol. Res. Gr.* **2005**, *30*, 935–953. [CrossRef]
74. Hewawasam, T.; von Blanckenburg, F.; Schaller, M.; Kubik, P. Increase of human over natural erosion rates in tropical highlands constrained by cosmogenic nuclides. *Geology* **2003**, *31*, 597–600. [CrossRef]
75. Clapp, E.M.; Bierman, P.R.; Nichols, K.K.; Pavich, M.; Caffee, M. Rates of sediment supply to arroyos from upland erosion determined using in situ produced cosmogenic 10 Be and 26 Al. *Quat. Res.* **2001**, *55*, 235–245. [CrossRef]
76. Food and Agriculture Organization AQUASTAT. Global River Sediment Yields Database. Available online: http://www.fao.org/nr/water/aquastat/sediment/index.stm (accessed on 9 February 2019).
77. U. S. Department of the Interior Bureau of Reclamation Reclamation Library/Glossary. Available online: https://www.usbr.gov/library/glossary/ (accessed on 12 July 2019).
78. Strand, R.I.; Pemberton, E.L. *Reservoir Sedimentation: Technical Guideline for Bureau of Reclamation*; Bureau of Reclamation: Denver, CO, USA, 1982.
79. U.S. Department of Agriculture Soil Conservation Service. *Sediment Sources, Yields, Ratios. Chapter 6 in National Engineering Handbook, Section 3, Sedimentation*; U.S. Department of Agriculture Soil Conservation Service: Washington, DC, USA, 1983.
80. Wischmeier, W.H.; Smith, D.D. Predicting rainfall erosion losses from cropland. *USDA Agric. Handb.* **1965**, *282*.
81. Borrelli, P.; Van Oost, K.; Meusburger, K.; Alewell, C.; Lugato, E.; Panagos, P. A step towards a holistic assessment of soil degradation in Europe: Coupling on-site erosion with sediment transfer and carbon fluxes. *Environ. Res.* **2018**, *161*, 291–298. [CrossRef] [PubMed]
82. Wischmeier, W.H.; Smith, D.D. *Predicting Rainfall Erosion Losses—A Guide to Conservation Planning*; Agriculture Handbook No. 537; U.S. Department of Agriculture: Washington, DC, USA, 1978.
83. Arnold, J.G.; Srinivasan, R.; Muttiah, R.S.; Williams, J.R. Large area hydrologic modeling and assessment part I: Model development 1. *JAWRA J. Am. Water Resour. Assoc.* **1998**, *34*, 73–89. [CrossRef]
84. Young, R.A.; Onstad, C.A.; Bosch, D.D.; Anderson, W.P. AGNPS: A nonpoint-source pollution model for evaluating agricultural watersheds. *J. Soil Water Conserv.* **1989**, *44*, 168–173.
85. Laflen, J.M.; Lane, L.J.; Foster, G.R. WEPP: A new generation of erosion prediction technology. *J. Soil Water Conserv.* **1991**, *46*, 34–38.
86. Gellis, A.C.; Pavich, M.J.; Bierman, P.R.; Clapp, E.M.; Ellevein, A.; Aby, S. Modern sediment yield compared to geologic rates of sediment production in a semi-arid basin, New Mexico: Assessing the human impact. *Earth Surf. Process. Landf. J. Br. Geomorphol. Res. Gr.* **2004**, *29*, 1359–1372. [CrossRef]
87. Larson, P.H.; Dorn, R.I.; Skotnicki, S.J.; Seong, Y.B.; Jeong, A.; DePonty, J. Impact of drainage integration on basin geomorphology and landform evolution: A case study along the Salt and Verde rivers, Sonoran Desert, USA. *Geomorphology* **2020**, *371*, 107439. [CrossRef]

88. Vanmaercke, M.; Poesen, J.; Broeckx, J.; Nyssen, J. Sediment yield in Africa. *Earth Sci. Rev.* **2014**, *136*, 350–368. [CrossRef]
89. Vanmaercke, M.; Poesen, J.; Maetens, W.; de Vente, J.; Verstraeten, G. Sediment yield as a desertification risk indicator. *Sci. Total Environ.* **2011**, *409*, 1715–1725. [CrossRef]
90. Harel, M.-A.; Mudd, S.M.; Attal, M. Global analysis of the stream power law parameters based on worldwide 10Be denudation rates. *Geomorphology* **2016**, *268*, 184–196. [CrossRef]
91. Pulido, M.; Schnabel, S.; Lavado Contador, J.F.; Lozano-Parra, J.; Gómez-Gutiérrez, Á.; Brevik, E.C.; Cerdà, A. Reduction of the frequency of herbaceous roots as an effect of soil compaction induced by heavy grazing in rangelands of SW Spain. *CATENA* **2017**, *158*, 381–389. [CrossRef]
92. Pulido, M.; Barrena-González, J.; Badgery, W.; Rodrigo-Comino, J.; Cerdà, A. Sustainable grazing. *Curr. Opin. Environ. Sci. Heal.* **2018**, *5*, 42–46. [CrossRef]
93. Antoneli, V.; Rebinski, E.A.; Bednarz, J.A.; Rodrigo-Comino, J.; Keesstra, S.D.; Cerdà, A.; Pulido Fernández, M. Soil Erosion Induced by the Introduction of New Pasture Species in a Faxinal Farm of Southern Brazil. *Geosciences* **2018**, *8*, 166. [CrossRef]
94. Yibeltal, M.; Tsunekawa, A.; Haregeweyn, N.; Adgo, E.; Meshesha, D.T.; Aklog, D.; Masunaga, T.; Tsubo, M.; Billi, P.; Vanmaercke, M.; et al. Analysis of long-term gully dynamics in different agro-ecology settings. *CATENA* **2019**, *179*, 160–174. [CrossRef]
95. Fenta, A.A.; Tsunekawa, A.; Haregeweyn, N.; Poesen, J.; Tsubo, M.; Borrelli, P.; Panagos, P.; Vanmaercke, M.; Broeckx, J.; Yasuda, H.; et al. Land susceptibility to water and wind erosion risks in the East Africa region. *Sci. Total Environ.* **2020**, *703*, 135016. [CrossRef]
96. Dastgheyb Shirazi, S.S.; Ahmadi, A.; Abdi, N.; Toranj, H.; Khaleghi, M.R. Long-term grazing exclosure: Implications on water erosion and soil physicochemical properties (case study: Bozdaghin rangelands, North Khorasan, Iran). *Environ. Monit. Assess.* **2021**, *193*, 51. [CrossRef] [PubMed]
97. Whitley, D.S. Rock Art Dating and the Peopling of the Americas. *J. Archaeol.* **2013**, *2013*, 713159. [CrossRef]
98. Whitley, D.S.; Dorn, R.I. New Perspectives on the Clovis vs. Pre-Clovis Controversy. *Am. Antiq.* **1993**, *58*, 626–647. [CrossRef]
99. McAuliffe, J.R.; Van Devender, T.R. A 22,000-year record of vegetation change in the north-central Sonoran Desert. *Palaeogeogr. Palaeoclimatol. Palaeoecol.* **1998**, *141*, 253–275. [CrossRef]
100. Staley, S.E.; Fawcett, P.J.; Anderson, R.S.; Jiménez-Moreno, G. Early Pleistocene−to−present paleoclimate archive for the American Southwest from Stoneman Lake, Arizona, USA. *GSA Bull.* **2021**. [CrossRef]
101. Cerdà, A. The Role of Fire in Achieving the Sustainable Development Goals of the United Nations. *Multidiscip. Digit. Publ. Inst. Proc.* **2019**, *30*, 65. [CrossRef]
102. Dindaroglu, T.; Babur, E.; Yakupoglu, T.; Rodrigo-Comino, J.; Cerdà, A. Evaluation of geomorphometric characteristics and soil properties after a wildfire using Sentinel-2 MSI imagery for future fire-safe forest. *Fire Saf. J.* **2021**, *122*, 103318. [CrossRef]
103. Fernández-Raga, M.; Gutiérrez, E.G.; Keesstra, S.D.; Tárrega, R.; Nunes, J.P.; Marcos, E.; Rodrigo-Comino, J. Determining the potential impacts of fire and different land uses on splash erosion in the margins of drylands. *J. Arid Environ.* **2021**, *186*, 104419. [CrossRef]
104. Portenga, E.W.; Rood, D.H.; Bishop, P.; Bierman, P.R. A late holocene onset of aboriginal burning in southeastern Australia. *Geology* **2016**, *44*, 131–134. [CrossRef]
105. Wolman, M.G. A cycle of sedimentation and erosion in urban river channels. *Geogr. Ann. Ser. A Phys. Geogr.* **1967**, *49*, 385–395. [CrossRef]
106. Roberts, W.P.; Pierce, J.W. Sediment yield in the Patuxent River (Md.) undergoing urbanization, 1968–1969. *Sediment. Geol.* **1974**, *12*, 179–197. [CrossRef]
107. Cerdà, A. Effects of rock fragment cover on soil infiltration, interrill runoff and erosion. *Eur. J. Soil Sci.* **2001**, *52*, 59–68. [CrossRef]
108. Seong, Y.B.; Dorn, R.I.; Yu, B.Y. Evaluating the life expectancy of a desert pavement. *Earth Sci. Rev.* **2016**, *162*, 129–154. [CrossRef]
109. Borrelli, P.; Robinson, D.A.; Fleischer, L.R.; Lugato, E.; Ballabio, C.; Alewell, C.; Meusburger, K.; Modugno, S.; Schütt, B.; Ferro, V.; et al. An assessment of the global impact of 21st century land use change on soil erosion. *Nat. Commun.* **2017**, *8*, 2013. [CrossRef]
110. Baker, D.L.; King, K.A. *Environmental Contaminant Investigation of Water Quality, Sediment and Biota of the Upper Gila River Basin, Arizona*; U.S. Fish and Wildlife Service Arizona Ecological Services State Office: Phoenix, AZ, USA, 1994.
111. Zhuo, X.; Boone, C.G.; Shock, E.L. Soil lead distribution and environmental justice in the Phoenix metropolitan region. *Environ. Justice* **2012**, *5*, 206–213. [CrossRef]
112. Li, G.; Sun, G.-X.; Ren, Y.; Luo, X.-S.; Zhu, Y.-G. Urban soil and human health: A review. *Eur. J. Soil Sci.* **2018**, *69*, 196–215. [CrossRef]
113. Pribadi, D.O.; Vollmer, D.; Pauleit, S. Impact of peri-urban agriculture on runoff and soil erosion in the rapidly developing metropolitan area of Jakarta, Indonesia. *Reg. Environ. Chang.* **2018**, *18*, 2129–2143. [CrossRef]
114. Langemeyer, J.; Madrid-Lopez, C.; Mendoza Beltran, A.; Villalba Mendez, G. Urban agriculture—A necessary pathway towards urban resilience and global sustainability? *Landsc. Urban Plan.* **2021**, *210*, 104055. [CrossRef]
115. Scharenbroch, B.; Day, S.; Trammell, T.; Pouyat, R. Urban soil carbon storage. In *Urban Soils*; CRC Press: Boca Raton, FL, USA, 2017; pp. 137–154, ISBN 1315154250.
116. Vasenev, V.; Kuzyakov, Y. Urban soils as hot spots of anthropogenic carbon accumulation: Review of stocks, mechanisms and driving factors. *Land Degrad. Dev.* **2018**, *29*, 1607–1622. [CrossRef]
117. Sanderman, J.; Berhe, A.A. The soil carbon erosion paradox. *Nat. Clim. Chang.* **2017**, *7*, 317–319. [CrossRef]

118. Richter, D.D. Game Changer in Soil Science. The Anthropocene in soil science and pedology. *J. Plant Nutr. Soil Sci.* **2020**, *183*, 5–11. [CrossRef]
119. Cendrero, A.; Forte, L.M.; Remondo, J.; Cuesta-Albertos, J.A. Anthropocene Geomorphic Change. Climate or Human Activities? *Earth's Future* **2020**, *8*, e2019EF001305. [CrossRef]
120. Steffen, W.; Rockström, J.; Richardson, K.; Lenton, T.M.; Folke, C.; Liverman, D.; Summerhayes, C.P.; Barnosky, A.D.; Cornell, S.E.; Crucifix, M.; et al. Trajectories of the Earth System in the Anthropocene. *Proc. Natl. Acad. Sci. USA* **2018**, *115*, 8252–8259. [CrossRef] [PubMed]
121. Nyssen, J.; Poesen, J.; Moeyersons, J.; Haile, M.; Deckers, J. Dynamics of soil erosion rates and controlling factors in the Northern Ethiopian Highlands—towards a sediment budget. *Earth Surf. Process. Landf.* **2008**, *33*, 695–711. [CrossRef]
122. Rodrigo Comino, J.; Iserloh, T.; Lassu, T.; Cerdà, A.; Keestra, S.D.; Prosdocimi, M.; Brings, C.; Marzen, M.; Ramos, M.C.; Senciales, J.M.; et al. Quantitative comparison of initial soil erosion processes and runoff generation in Spanish and German vineyards. *Sci. Total Environ.* **2016**, *565*, 1165–1174. [CrossRef]
123. Haregeweyn, N.; Tsunekawa, A.; Poesen, J.; Tsubo, M.; Meshesha, D.T.; Fenta, A.A.; Nyssen, J.; Adgo, E. Comprehensive assessment of soil erosion risk for better land use planning in river basins: Case study of the Upper Blue Nile River. *Sci. Total Environ.* **2017**, *574*, 95–108. [CrossRef]
124. Cerdà, A.; Rodrigo-Comino, J.; Giménez-Morera, A.; Keesstra, S.D. An economic, perception and biophysical approach to the use of oat straw as mulch in Mediterranean rainfed agriculture land. *Ecol. Eng.* **2017**, *108*, 162–171. [CrossRef]
125. Yu, Y.; Rodrigo-Comino, J. Analyzing Regional Geographic Challenges: The Resilience of Chinese Vineyards to Land Degradation Using a Societal and Biophysical Approach. *Land* **2021**, *10*, 227. [CrossRef]
126. Verheijen, F.G.A.; Jones, R.J.A.; Rickson, R.J.; Smith, C.J. Tolerable versus actual soil erosion rates in Europe. *Earth Sci. Rev.* **2009**, *94*, 23–38. [CrossRef]
127. Keesstra, S.D.; Bouma, J.; Wallinga, J.; Tittonell, P.; Smith, P.; Cerdà, A.; Montanarella, L.; Quinton, J.N.; Pachepsky, Y.; van der Putten, W.H.; et al. The significance of soils and soil science towards realization of the United Nations Sustainable Development Goals. *SOIL* **2016**, *2*, 111–128. [CrossRef]
128. Cerdà, A.; Keesstra, S.D.; Rodrigo-Comino, J.; Novara, A.; Pereira, P.; Brevik, E.; Giménez-Morera, A.; Fernández-Raga, M.; Pulido, M.; di Prima, S.; et al. Runoff initiation, soil detachment and connectivity are enhanced as a consequence of vineyards plantations. *J. Environ. Manag.* **2017**, *202*, 268–275. [CrossRef]